Large-scale connectivity of fluvio-deltaic stratigraphy

Inferences from simulated accommodation-to-supply cycles and automated extraction of chronosomes

Karamitopoulos, Pantelis; Weltje, Gert J.; Dalman, Rory A.F.

DOI
10.1111/bre.12471

Publication date
2020

Document Version
Final published version

Published in
Basin Research

Citation (APA)
Karamitopoulos, P., Weltje, G. J., & Dalman, R. A. F. (2020). Large-scale connectivity of fluvio-deltaic stratigraphy: Inferences from simulated accommodation-to-supply cycles and automated extraction of chronosomes. *Basin Research*, *33*(1), 382-402. https://doi.org/10.1111/bre.12471

Received: 19 September 2019 | Revised: 2 May 2020 | Accepted: 7 May 2020

DOI: 10.1111/bre.12471

ORIGINAL ARTICLE

Basin Research | IAS EAGE | WILEY

Large-scale connectivity of fluvio-deltaic stratigraphy: Inferences from simulated accommodation-to-supply cycles and automated extraction of chronosomes

Pantelis Karamitopoulos[1] | **Gert J. Weltje**[2] | **Rory A. F. Dalman**[3]

[1]Department of Geoscience and Engineering, Delft University of Technology, Delft, Netherlands

[2]Division of Geology, Department of Earth and Environmental Sciences, KU Leuven, Leuven, Belgium

[3]Geological Survey of the Netherlands, TNO, Utrecht, Netherlands

Correspondence
Pantelis Karamitopoulos, Department of Geoscience and Engineering, Delft University of Technology, Stevinweg 1, NL-2628CN Delft, Netherlands.
Email: p.karamitopoulos@tudelft.nl

Abstract

Multiscale simulation of fluvio-deltaic stratigraphy was used to quantify the elements of the geometry and architectural arrangement of sub-seismic-scale fluvial-to-shelf sedimentary segments. We conducted numerical experiments of fluvio-deltaic system evolution by simulating the accommodation-to-sediment-supply (A/S) cycles of varying wavelength and amplitude with the objective to produce synthetic 3-D stratigraphic records. Post-processing routines were developed in order to investigate delta lobe architecture in relation to channel-network evolution throughout A/S cycles, estimate net sediment accumulation rates in 3-D space, and extract chronostratigraphically constrained lithosomes (or chronosomes) to quantify large-scale connectivity, that is, the spatial distribution of high net-to-gross lithologies. Chronosomes formed under the conditions of channel-belt aggradation are separated by laterally continuous abandonment surfaces associated with major avulsions and delta-lobe switches. Chronosomes corresponding to periods in which sea level drops below the inherited shelf break, that is, the youngest portions of the late falling stage systems tract (FSST), form in the virtual absence of major avulsions, owing to the incision in their upstream parts, and thus display purely degradational architecture. Detailed investigation of chronosomes within the late FSST showed that their spatial continuity may be disrupted by higher-frequency A/S cycles to produce "stranded" sand-rich bodies encased in shales. Chronosomes formed during early and late falling stage (FSST) demonstrate the highest large-scale connectivity in their proximal and distal areas, respectively. Lower-amplitude base level changes, representative of greenhouse periods during which the shelf break is not exposed, increase the magnitude of delta-lobe switching and favour the development of system-wide abandonment surfaces, whose expression in real-world stratigraphy is likely to reflect the intertwined effects of high-frequency allogenic forcing and differential subsidence.

KEYWORDS

A/S cycle, abandonment surface, avulsion, chronosome, connectivity, process stratigraphy, sediment accumulation rate

The peer review history for this article is available at https://publons.com/publon/10.1111/bre.12471

1 | INTRODUCTION

Process (dynamic or genetic) stratigraphy studies the dynamics of the controls on basin-fill segments, that is, the rate and spatial distribution of accommodation and sediment supply (where the latter is specified in terms of volume and grain-size distribution) (Allen & Allen, 2013; Cross, 1990; Galloway, 1989; Matthews, 1974). The interplay between these factors at different spatio-temporal scales is responsible for the generation of siliciclastic basin-fill segments with distinct aggradational, progradational, degradational and/or retrogradational stratal geometries (Catuneanu et al., 2009; Emery & Myers, 1996; Frazier, 1974; Galloway, 1975, 1989; Helland-Hansen & Hampson, 2009; Neal & Abreu, 2009). The aim of the process stratigraphy is to infer allogenic forcing and autogenic processes from stratal geometries and cycles found in sedimentary basins (Barrell, 1917; Miall, 2010; Tipper, 2000). The process stratigraphic approach is similar to the "standardised" sequence stratigraphic approach which stresses the genetic structure of stratigraphy as a function of accommodation and sediment supply (Catuneanu et al., 2009). While the latter is purely observational (Catuneanu, 2020), process stratigraphy "is essentially a mass or volume balance exercise" (Allen & Allen, 2013) that utilizes physical and numerical experimentation to understand the effects of processes on stratal geometries at different spatio-temporal scales (Burgess, Lammers, Van Oosterhout, & Granjeon, 2006; Burgess, Allen, & Steel, 2016; Burgess & Prince, 2015; Martin, Paola, Abreu, Neal, & Sheets, 2009; Paola, 2000; Paola, Heller, & Angevine, 1992; Paola, Straub, Mohrig, & Reinhardt, 2009; Pellegrini, Patruno, Helland-Hansen, Steel, & Trincardi, 2020; Ritchie, Gawthorpe, & Hardy, 2004a, 2004b; Sheets, Hickson, & Paola, 2002; Zhang, Burgess, Granjeon, & Steel, 2019).

The fundamental notions of sequence stratigraphy resulted from the observations of conspicuous patterns on continental-margin seismic lines (Mitchum, Vail, & Thompson, 1977; Payton, 1977; Vail, Mitchum, & Thompson, 1977). In this context, seismic reflection events are interpreted to outline basin-fill segments whose architectural arrangement is regulated by the base-level changes. This perspective has forged a series of 2-D sequence stratigraphic models which have been customarily used to subdivide sedimentary sequences into genetically related units aiming at the landward and basinward prediction of lithological composition and reservoir potential (Catuneanu et al., 2009; Embry, 1995; Galloway, 1989; Helland-Hansen & Hampson, 2009; Hunt & Tucker, 1992; Neal & Abreu, 2009; Plint & Nummedal, 2000; Posamentier & Allen, 1999; Posamentier & Vail, 1988; Ridente, 2016; Shanley & McCabe, 1993; Wright & Marriott, 1993). Due to the fact that these models are qualitative and cannot be easily verified, there exists a genuine need to: (1) accurately estimate net sediment accumulation rates; (2) provide quantifiable information regarding the processes acting throughout an accommodation to sediment supply (A/S) cycle; (3) expand sequence stratigraphic analysis to three dimensions in order to improve lithology prediction (Bhattacharya, 2011; Burgess, 2016; Dalman, Weltje, & Karamitopoulos, 2015; Emery & Myers, 1996; Griffiths, 1996; Griffiths & Nordlund, 1993; Hampson, 2016; Holbrook & Bhattacharya, 2012; Karamitopoulos, Weltje, & Dalman, 2014; Madof, Harris, & Connell, 2016; Martinius, Elfenbein, & Keogh, 2014; Miall, 2014; Muto & Steel, 1997, 2004; Muto, Steel, & Burgess, 2016; Ritchie et al., 2004a, 2004b; Sadler, 1981; Sadler & Strauss, 1990; Tipper, 2015, 2016).

Stratigraphic forward models (SFMs) are well-suited for addressing each of the above issues as they permit investigation of the morphodynamic evolution of sediment dispersal systems over a wide range of temporal and spatial scales and provide synthetic stratigraphy at a resolution comparable to subsurface data (Burgess, 2012; Charvin Gallagher, Hampson, & Labourdette, 2009; Cross & Lessenger, 1999; Dalman & Weltje, 2008, 2012; Falivene et al., 2014; Granjeon & Joseph, 1999; Hajek & Wolinsky, 2012; Imhof & Sharma, 2006; Karssenberg, Törnqvist, & Bridge, 2001; Karssenberg, De Vries, & Bridge, 2007; Meijer, 2002; Paola, 2000; Wijns, Poulet, Boschetti, Dyt, & Griffiths, 2004). A widely used approach to model clastic sedimentary systems is based on topographic diffusion, which can be combined with advective transport to represent the channelized flow (e.g., Granjeon, 2014; Granjeon & Joseph, 1999; Hajek & Wolinsky, 2012; Harris, Covault, Baumgardner, Sun, & Granjeon, 2020; Meijer, 2002). This approach cannot provide detailed sedimentological heterogeneity at the sub-seismic scale. Sub-seismic heterogeneity can only be captured by basin-scale models in which small-scale processes are represented by sub-grid elements, such as SimClast (Dalman

Highlights

- A process-based forward stratigraphic model was used to simulate accommodation-to-sediment supply (A/S) cycles of varying wavelength and amplitude.
- A post-processing software suite was developed to extract chronostratigraphically constrained lithosomes (or chronosomes).
- The linkage between avulsion events and A/S cycles is documented.
- Chronosomes formed during early and late falling stage (FSST) demonstrate the highest large-scale connectivity in their proximal and distal areas, respectively.

& Weltje, 2008, 2012), or by process-based models that involve the direct coupling of sediment transport and hydrodynamics, such as Delft3D (http://oss.deltares.nl/web/delft3d) and Sedsim (Griffiths, 1996; Martinez & Harbaugh, 1993; Tetzlaff & Harbaugh, 1989). Models of the former type are also known as aggregated models because they employ a high level of abstraction in order to ensure computational efficiency. Those of the latter type is more complex and hence come with high computational overhead during simulation, which renders them as yet unsuitable for exploring the inherent uncertainty of initial and boundary conditions through multiple runs.

In this study, we focused on the role of sedimentation processes, specifically avulsions, in the formation and architectural arrangement of river-shelf sedimentary segments throughout a sequence, that is, a cycle of accommodation to sediment supply rates (Neal & Abreu, 2009), which may be viewed as a natural stratigraphic unit (Catuneanu et al., 2009, 2011; Karamitopoulos et al., 2014). For this purpose, we used SimClast, a basin-scale numerical model with a sub-grid parameterization of fluvio-deltaic processes and stratigraphy. Standard sequence stratigraphic terminology, including the concept of accommodation to sediment supply (A/S) ratio based on the regime theory of Swift and Thorne (1991) and Thorne and Swift (1991), was used for the analysis and interpretation of the results. A routine was implemented to extract chronosomes, short for chronostratigraphically constrained lithosomes (Schultz, 1982) from the synthetic stratigraphic records preserved throughout an A/S cycle. Chronosomes consist of channel-belt and delta-lobe sediments deposited in temporal continuity at a specific location within the basin (Dalman et al., 2015; Schultz, 1982). The aims of this study are to (1) investigate channel-network evolution throughout A/S cycles of varying amplitude and wavelength, (2) estimate net sediment accumulation rates to capture the time evolution of deposition and storage of fluvial-shelf segments, and (3) provide a coherent predictive model of lithofacies distribution and large-scale connectivity throughout the simulated A/S cycles.

2 | METHODS

2.1 | Model description

SimClast, a basin-scale numerical model of river-shelf evolution (Meijer, 2002) combined with a sub-grid parameterization of fluvio-deltaic processes and stratigraphy (Dalman & Weltje, 2008, 2012) was used to obtain synthetic sedimentary sequences that form under the influence of time-variant external forcing in the form of sea-level cycles on a uniformly subsiding (0.1 mm/yr) substrate resembling a passive margin with a well-developed shelf and a clearly defined shelf break (model domain is 50 × 100 km) (Figure 1). The adopted grid-cell size of 1 × 1 km represents the finest spatial discretization at which the model can operate, because the grid-cell size needs to be larger than the width of an individual channel. Sedimentary processes relevant to this study are included by the sub-grid parameterization of in-channel sediment transport able to produce divergent (aggrading: braided or meandering) and convergent (incising) channel networks, and most importantly, detailed representations of avulsions and mouth bar-induced bifurcations. Avulsions occur as a consequence of channel-belt aggradation (e.g., through base level rise) and resulting super-elevation, whereas mouth bar-induced bifurcations dominate the terminal parts of the sediment dispersal system where delta lobes prograde and topographic gradients are low. Fluvio-deltaic evolution in the model has been shown (Dalman et al., 2015) to be governed by a robust morphodynamic feedback loop under time-invariant forcing, which links the progradation rate with major avulsions, delta-lobe switches, and sequestration of sediments on the delta plain. It is expected that this feedback loop is influenced by external forcing, and therefore stratigraphic records formed under time-variant forcing conditions are presented in this study. Throughout the model runs, the net sediment accumulation record ($d(t_k)$) was stored in dynamic arrays to register deposition ($d(t_k) > 0$), erosion ($d(t_k) < 0$), and stasis ($d(t_k) = 0$) for every grid cell throughout the simulation. A grid cell in stasis (which does not change its elevation) is in bypass if the site is occupied by an active channel or starved if the grid cell is far away from the active channel (Tipper, 2000, 2015).

2.2 | Scenarios

In order to maximize the preservation potential of modelled delta-topset areas, all simulations were run in the absence of differential subsidence, coastal processes (i.e., waves, tides, cross-shore transport), and bank-stabilizing vegetation. The initial topographic surface for all simulations was defined by running the model for 20 kyr under time-invariant forcing (Figure 1a). Throughout the simulations, constant water discharge ($Q_w = 5 \times 10^9$ m^3/yr) and sediment input ($Q_s = 1 \times 10^6$ m^3/yr) (sand/clay ratio = 0.2) entered the transfer valley via a single entry point (Figure 1a). Two sets of numerical experiments were performed (Table 1): the first set consisted of 200-kyr model runs using low- and high-amplitude sea-level cycles representative of greenhouse and icehouse periods, respectively (experiments RC1 and RC2; Figure 1b, green and blue curves, respectively) (Miller et al., 2005). The crucial difference between the two scenarios is that in the former, the sea level does not fall below the shelf break, whereas the shelf break is periodically exposed

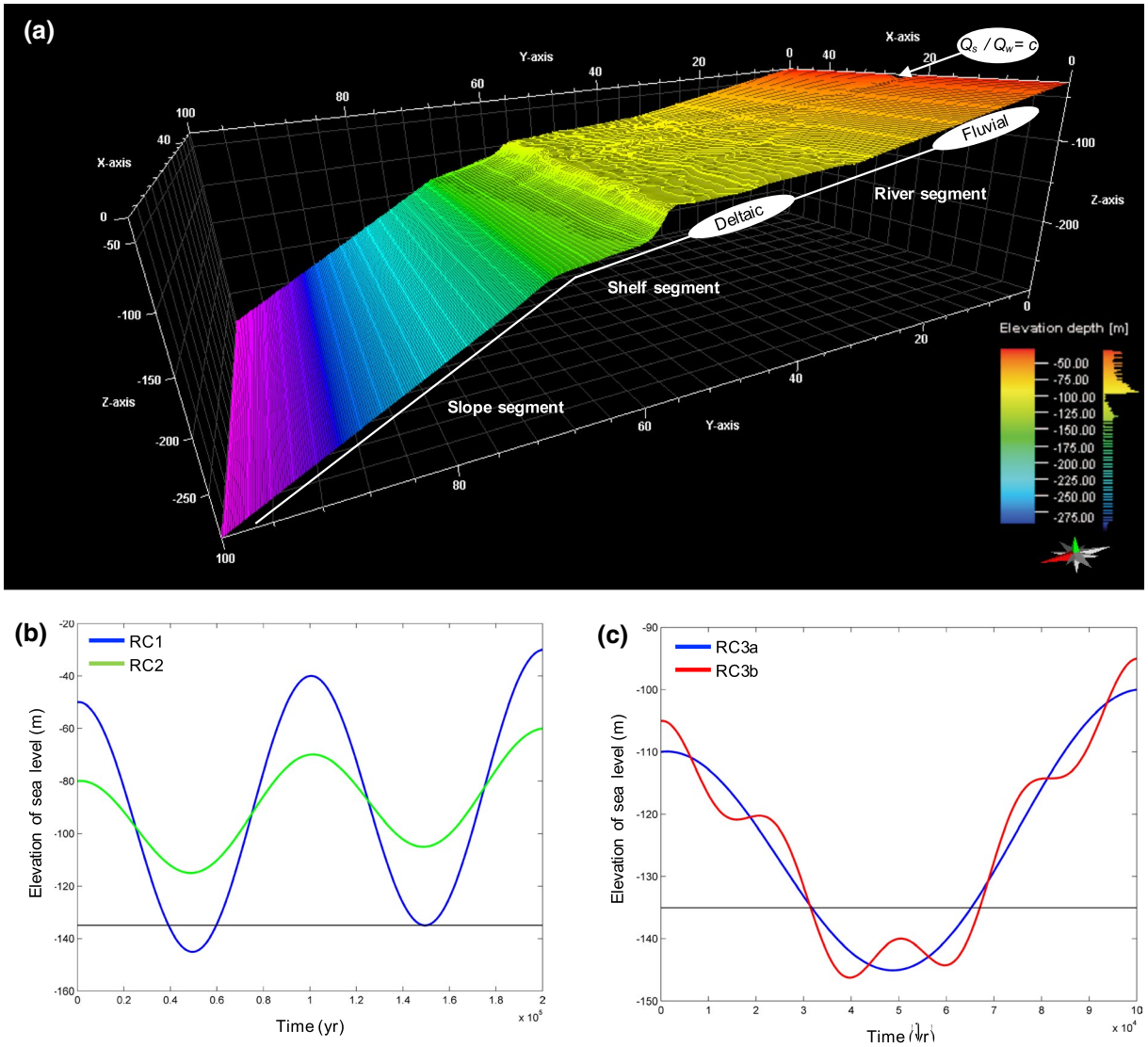

FIGURE 1 (a) Initial model topography and inflow point (white arrow); relative sea-level curves of the first (b) and the second set (c) of numerical experiments (black line in 1B indicates shelf break position). Scenario RC3 is the compound signal of RC3a and RC3b (see Table 1 for details)

in the latter. The second set of experiments consisted of 100-kyr model runs with a one-phase sea-level fall and rise with or without a superimposed higher frequency (25 kyr wavelength) signal (experiments RC3a and RC3b; Figure 1c, blue and red curves, respectively). The first set of experiments (RC1 and RC2) were aimed at the quantitative description of channel network and stratal architecture as a function of fixed topography and base level changes, whereas the second (RC3a and RC3b) focused on the architectural arrangement of sedimentary packages deposited during the periods of minimum A/S (i.e., falling stage systems tract or FSST for short). In order to quantify the variability of the synthetic stratigraphic records (captured in a probability distribution), 10 equiprobable realizations were obtained from the base-case scenario RC1 by applying random topographic noise to the initial surface.

TABLE 1 Reference base-level curves

Scenarios	Wavelength (kyr)	Amplitude (m)	Duration (kyr)
RC1 (base case)	100	50	200
RC2	100	15	200
RC3a	100	15	100
RC3b	25	10	100

2.3 | Post-processing

A stack data structure was designed and implemented as a linked list in C++ to load continuous records of synthetic stratigraphy (net sediment accumulation) in dynamic

arrays. The algorithm implements sequentially a series of post-processing methods that allow estimation of net sediment accumulation rates over specified time intervals to outline the boundaries of delta-lobe chronosomes (Figure 2). Figure 3 illustrates four delta lobes extracted from the base-case experiment, each covering a 2-kyr time interval. Large-scale connectivity has been quantified as the number of connected grid cells extracted by the cellular automata post-processing operation. In this particular application, connectivity represents the spatio-temporal continuity of high-net to gross fluvio-deltaic chronosomes. A detailed description of the methods is included in the Appendix A.

The dominant channel branches and their associated major avulsion sites occurring more than 5 km from coastline were extracted using the method described in detail by Karamitopoulos et al. (2014). The method involves a Boolean transformation of grid cells (channelized vs. non-channelized flow) based on a threshold discharge ($Q_{thr} = 3.0 \times 10^9$ m^3/yr) followed by a calculation of differences between Boolean channel networks at successive time steps. Major avulsions occurring more than 5 km away from coastline were identified at the intersection of the old and new channel branches (Figure 4). In addition, we estimated the Euclidian distance of the river-mouth shift owing to the major avulsion, which we named the magnitude of the delta-lobe switch (M_{DLS}). This metric is indicative of the impact of the major avulsions at the coastline.

2.4 | Stratigraphic terminology

The concept of accommodation to sediment supply (A/S) cycles (or sequences) provides an attractive way to analyse the morphodynamic evolution of fluvio-deltaic systems as a function of spatial and temporal patterns of sedimentation (Allen, Lang, Musakti, & Chirinos, 1996; Jervey, 1988; Martinius et al., 2014; Martinsen et al., 1999; Muto & Steel, 2002; Schlager, 1993; Shanley & McCabe, 1993; Thorne & Swift, 1991; Tipper, 2000). However, putting this concept into practice is not exactly straightforward owing to the fact that traditional sequence-stratigraphic definitions and naming conventions that stem from the 2-D world cannot be directly applied to real-world 3-D basin fills. Clarification and justification of the terms we employ is therefore in order.

The terminology of A/S cycles acknowledges the fact that A and S cannot be directly inferred from the stratigraphic record owing to its generally fragmentary nature (incomplete preservation) and limited time control, which implies incomplete knowledge of the past. The A/S ratio is a dimensionless number (a ratio of two rates) and thus by definition independent of time control. The A/S regime in the vicinity of the paleo-shoreline gives rise to unique stacking patterns (aggradational, degradational, progradational, and retrogradational; ADPR for short) that can be observed in the stratigraphic record. Thus, A/S > 1 results in the retrogradational stacking (which implies transgression), A/S = 1 results in aggradational stacking (which implies a stationary coastline),

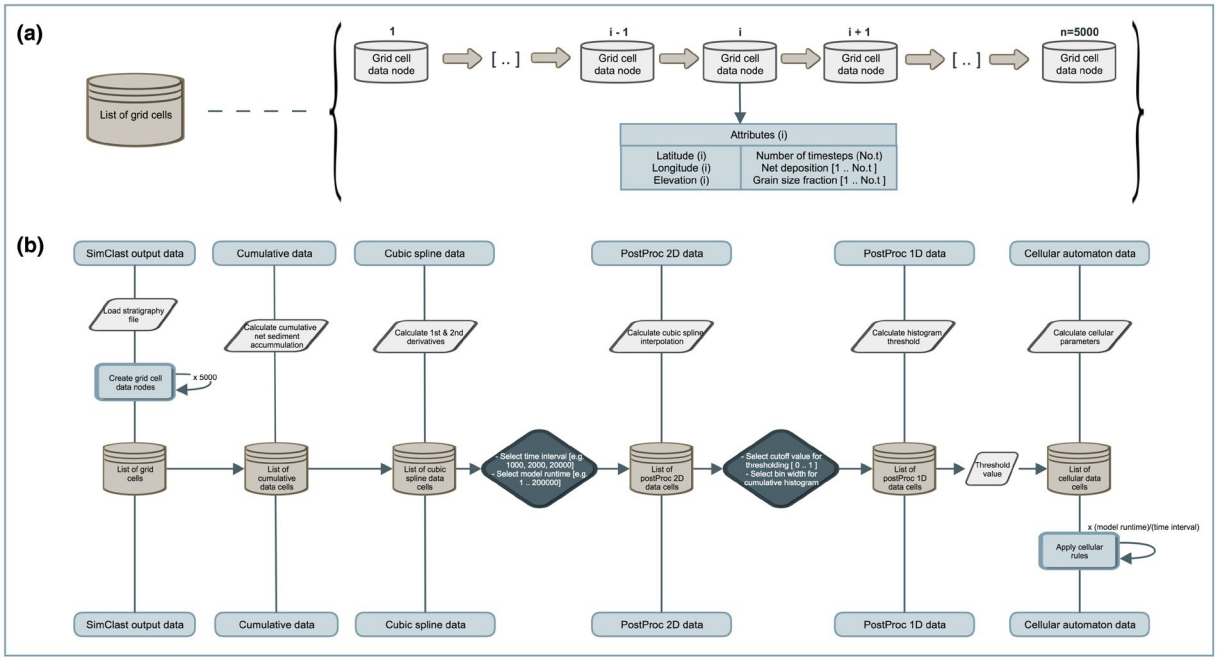

FIGURE 2 Flowchart illustrating the implementation of post-processing routines: (a) list of grid cells linked in a dynamic array structure; (b) generalized post-processor data flow. See Appendix A for full discussion

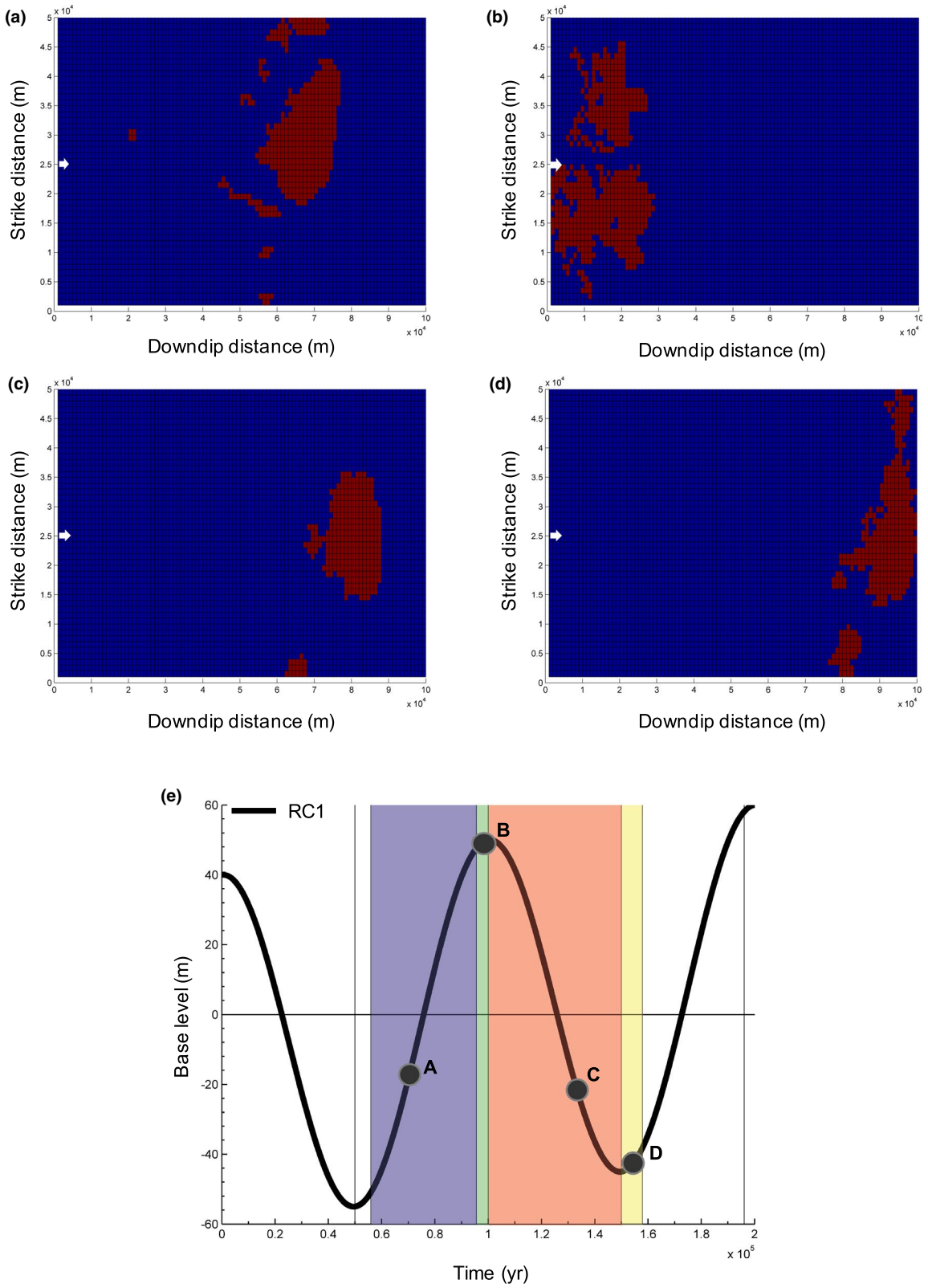

FIGURE 3 Examples of transgressive (a), (b) and regressive (c), (d) chronosomes (2 kyr) extracted from base-case scenario (RC1). White arrows indicate the location of the sediment entry point. (e) Normalized base-level curve: coloured intervals correspond to transgressive (blue), highstand (green), falling stage (red), and lowstand (yellow) systems tracts outlined sequentially by the correlative conformity (sensu Hunt & Tucker, 1992) maximum regressive surfaces, maximum flooding surfaces and the basal surface of forced regression (see Methods and Results sections for more details). Extracted chronosomes are marked by grey dots on the curve

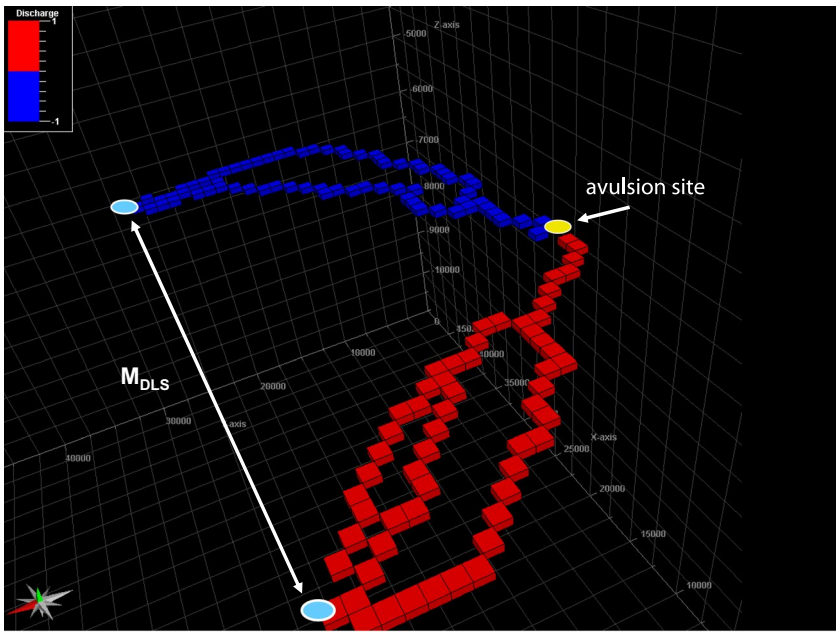

FIGURE 4 Channel network and automated extraction of major avulsion site (>5 km from coastline). Red and blue grid cells correspond to the abandoned and active channel, respectively. Magnitude of the delta-lobe switch (M_{DLS}) corresponds to river mouth shift distance at the coastline (modified from Karamitopoulos et al., 2014)

$0 < A/S < 1$ results in progradational stacking (which implies "normal" regression), and $A/S < 0$ results in degradational stacking (which implies "forced" regression).

Traditional sequence stratigraphic terminology mixes observation and interpretation, because changes in boundary conditions (which can only be inferred under certain assumptions) are directly employed in the naming of stratigraphic units (systems tracts). The terms regression and transgression refer to the basinward and landward movement of the shoreline, respectively, whereas the terms highstand and lowstand refer to the relative (not absolute) sea level. None of these quantities can be directly observed in the stratigraphic record, and therefore, using such terms to describe stratigraphic units is questionable. In light of these considerations, the historical naming of systems tracts is unfortunate and continues to create unnecessary confusion, as all of their names refer to unobservable phenomena: the movement of the shoreline ("transgressive" systems tract, or TST) or the sea level ("highstand" systems tract, or HST; "lowstand" systems tract, or LST; "falling stage" systems tract, or FSST).

The modern usage of systems tracts emphasizes their definition as physical rock bodies with observable characteristics, that is, bounding surfaces and internal architecture (Neal & Abreu, 2009), devoid of unnecessary interpretative connotations. Thus, it seems reasonable to refer to the LST as the PA-tract, the TST as the R-tract, the HST as the AP-tract, and the FSST as the D-tract. However, this is not (yet) widely accepted by the research community. In this study, we will stick to the use of conventional terms for systems tracts and their bounding surfaces, for the simple reason that there is no widely accepted neutral alternative for the genetic description of stratigraphy. Therefore, the stratigraphic record was subdivided into system tracts using conventional 2-D sequence stratigraphic concepts (Emery & Myers, 1996; Frazier, 1974; Galloway, 1989; Helland-Hansen & Martinsen, 1996; Hunt & Tucker, 1992; Neal & Abreu, 2009; Plint & Nummedal, 2000; Posamentier & Allen, 1999; Posamentier, Jervey, & Vail, 1988; Posamentier & Vail, 1988; Vail, 1987).

Another complication arises from the fact that the assumption that some of the bounding surfaces of systems tracts are isochronous is not generally valid. This is not a serious problem in the applications of sequence stratigraphy to the 2-D world, but it does complicate the distinction of bounding surfaces in 3-D. As an example, consider the case in which a prograding delta is flanked by two stretches of coastline subject to erosion, such that progradation and retrogradation occur at the same time in different parts of the system. Then there is a choice between two alternatives: (1) acknowledging the diachroneity of bounding surfaces to preserve the unique internal stacking patterns of systems tracts, or (2) regarding bounding surfaces as isochronous by definition, thus allowing some variability in stacking patterns within the basal and topmost parts of systems tracts. Because we conducted numerical simulations and thus had direct access to boundary conditions, we opted for the latter and defined the bounding surfaces of the systems tracts (with the exception of the sequence boundary) as system-wide isochronous surfaces separating sedimentary packages that have different stacking patterns on average. The bounding surfaces were defined as follows. Maxima and minima of the non-dimensional shoreline curve, that is, the ratio of marine to non-marine grid cells, corresponding to the ages of maximum flooding (MFS) and maximum regressive surfaces (MRS), respectively. This metric is similar in spirit to the shoreline approximation metric defined by Martin et al. (2009) for flume-tank fluvial experiments. The ages of the basal surface of forced regression

(BSFR) and the correlative conformity (CC, sensu Hunt & Tucker, 1992) correspond to the highest and lowest values of the base-level curve, respectively. These four chronostratigraphic surfaces allow us to uniquely subdivide sequences into systems tracts. We thus ignored the fact that in real-world stratigraphy, the actual surfaces will record a certain degree of diachroneity depending on differential subsidence and locally varying rates of sediment supply (Catuneanu et al., 2009; Madof et al., 2016).

3 | RESULTS

Figure 5 illustrates the morphodynamic evolution of the RC1, RC2, RC3a, and RC3b experiments. In the base case scenario (RC1), the sea-level fluctuation was modelled as a sinusoid with a wavelength of 100 kyr and an amplitude of 50 m, representative of Pleistocene glacio-eustatic sea-level fluctuations (Figure 5a). During the deposition of the early FSST, delta-plain aggradation and progradation are regulated by the rate of the relative sea-level fall as well as the shelf and river-profile gradients (Karamitopoulos et al., 2014). Widespread erosion occurs especially when the sea level drops below the shelf break. During the TST, progradation shifts to retrogradation, which favours the development of super-elevation of alluvial ridges of the active channels. This increases the probability of avulsion, which peaks around the transition from the TST to the HST, that is, around the maximum flooding surface or the maximum aggradation level (as defined by Martinius et al., 2014) at the turn-around from retrogradation to progradation. Shelf break exposure during basin-fill evolution in scenarios RC3a and RC3b results in similar morphodynamics and sedimentation patterns (Figure 5c,d). In contrast, during RC2 basin-fill evolution the shelf break is not exposed and sedimentation takes place in the absence of pronounced localized erosive features (i.e., shelf-edge canyons) (Figure 5b).

Subdivision into systems tracts by the extraction of bounding surfaces is illustrated for the base-case scenario (RC1) in Figure 6. The snapshots mark the times assigned to the upper bounding surfaces of the TST, HST, FSST, and LST (Figure 6a–d, respectively). Their lower bounding surfaces (MRS, MFS, BSFR, and CC, respectively) are marked in the same figure and correspond to the maxima and minima of the non-dimensional shoreline and base level-change curves as explained above. The durations of the systems tracts vary considerably: 40 kyr for the TST, 4 kyr for the HST, 50 kyr for the FSST, and 6 kyr for the LST. The system tracts display

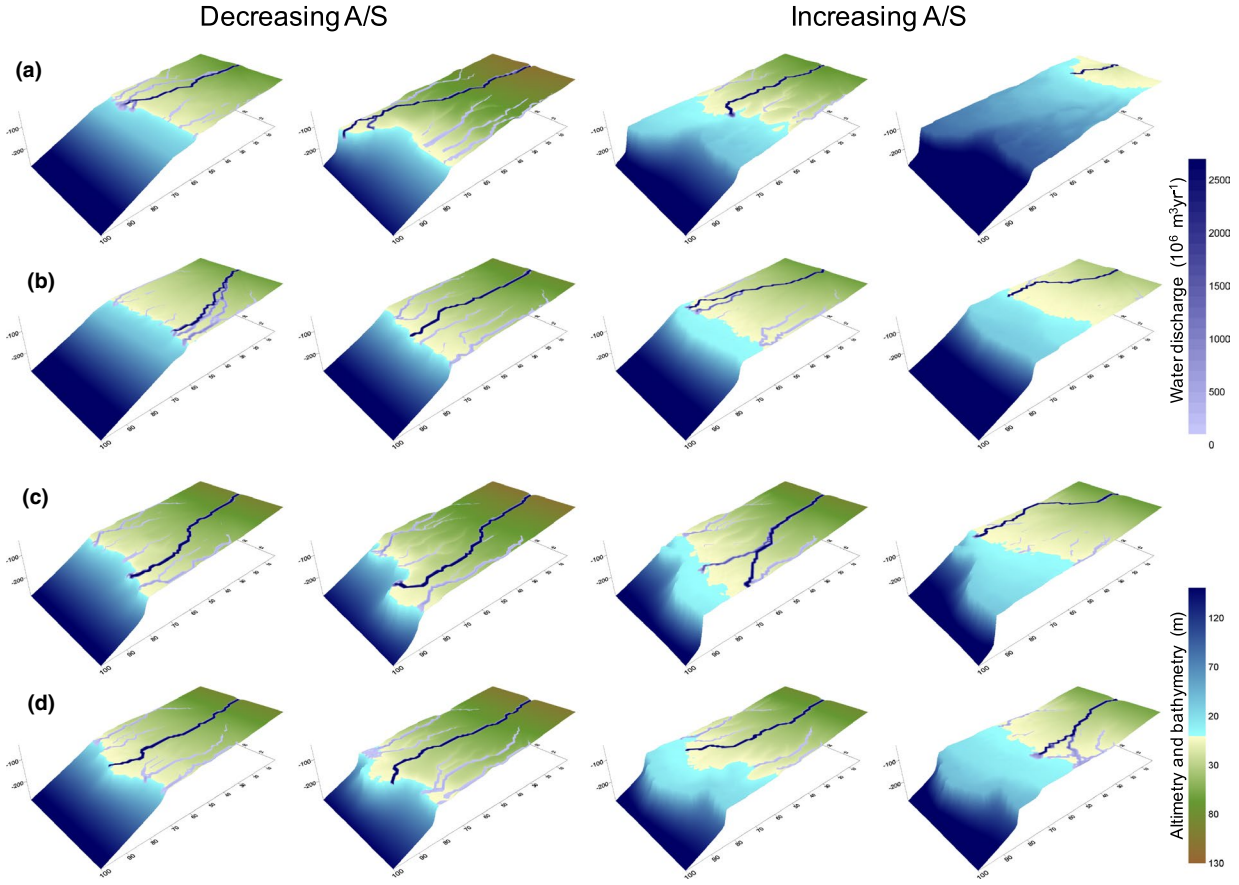

FIGURE 5 Morphological evolution (snapshots every 25 kyr) of experiment RC1 (a), RC2 (b), RC3a (c), and RC3b (d)

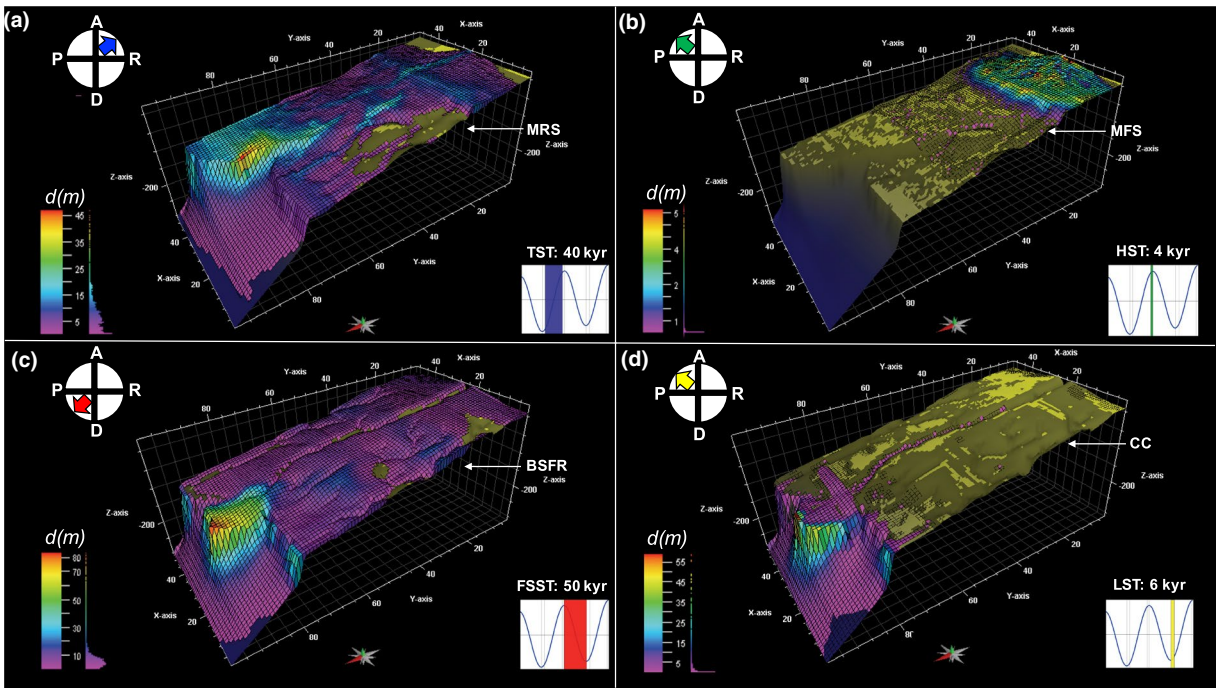

FIGURE 6 Thickness (m), duration, and ADPR stacking patterns of extracted: (a) transgressive systems tract (TST); (b) highstand systems tract (HST); (c) falling stage systems tract (FSST); (d) lowstand systems tract (LST)

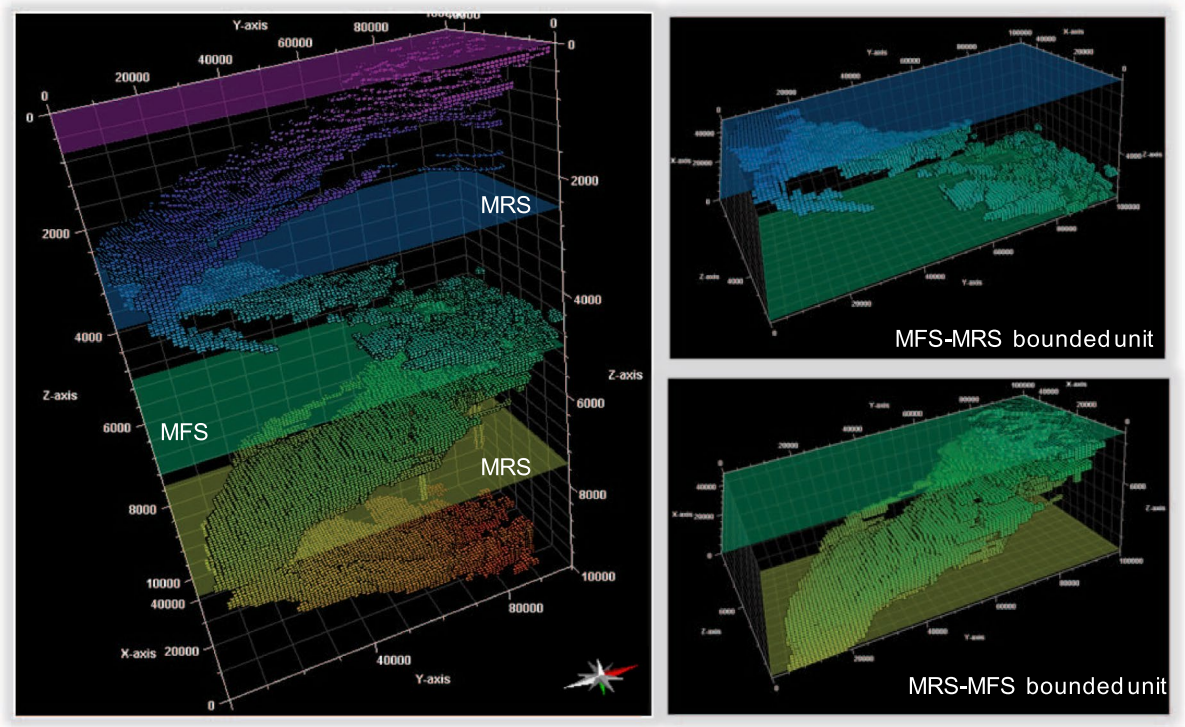

FIGURE 7 High-resolution sequence subdivision in the space-time (Wheeler) domain using automatically extracted chronosomes (1kyr resolution) (inverted)

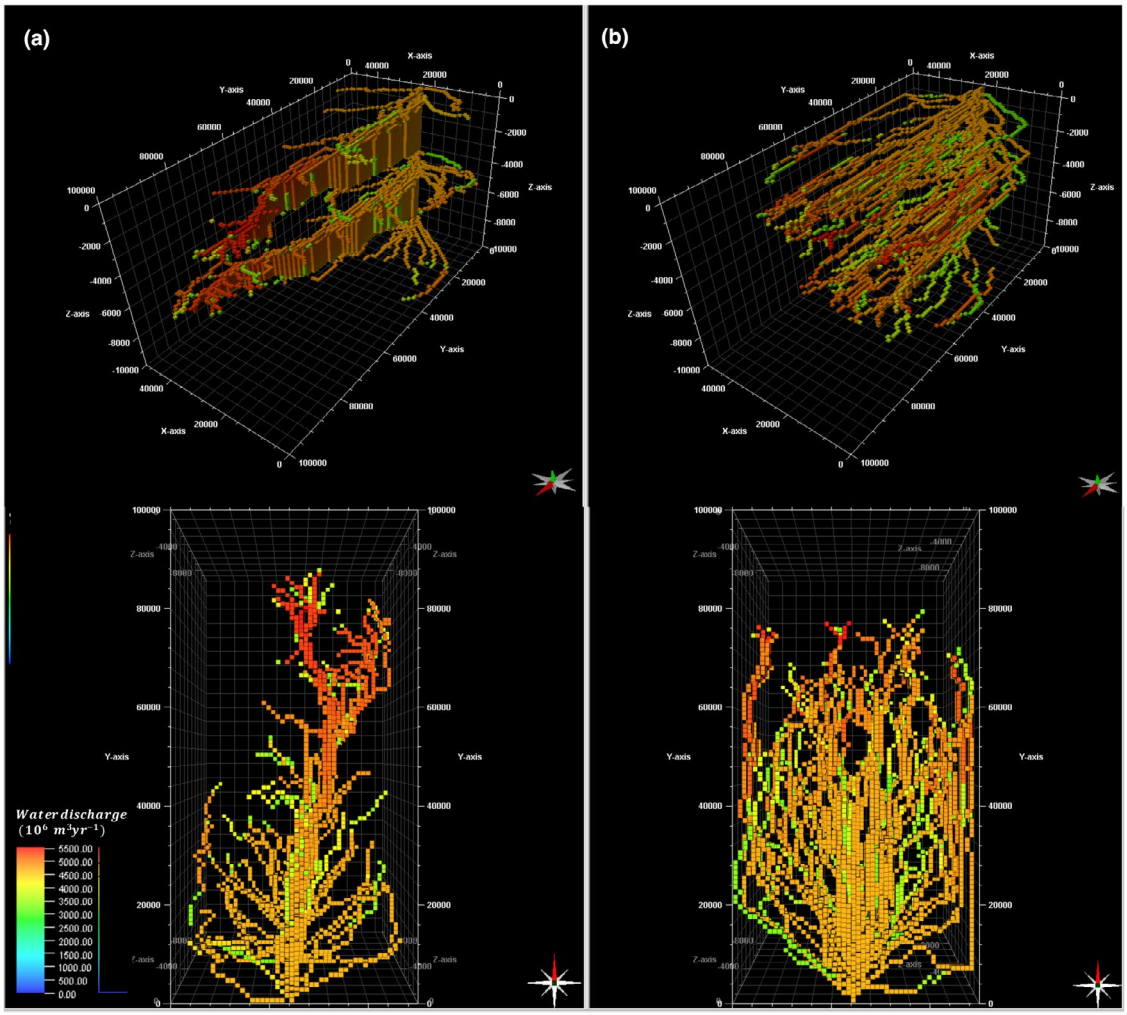

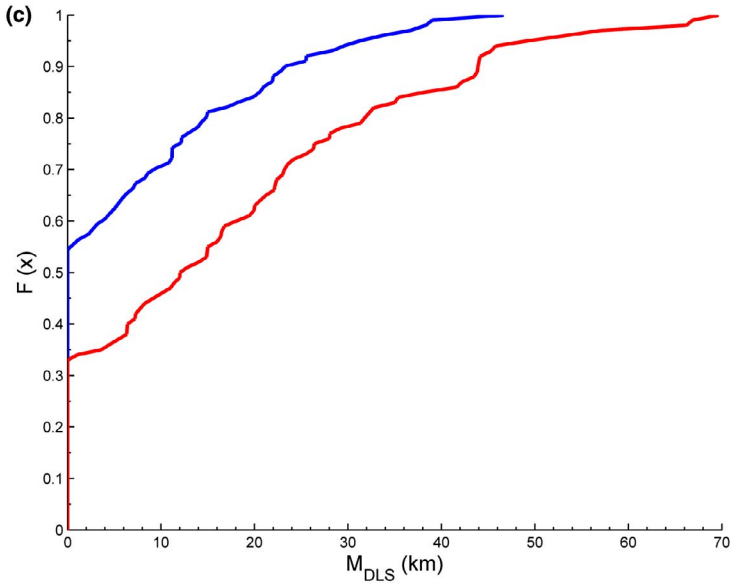

FIGURE 8 Cross-sectional and top views of the channelized drainage network in space-time (Wheeler) domain (2-kyr resolution) of RC1 (a) and RC2 (b) experiments. Channels exceed a threshold value of 3×10^9 m^3/yr. (c) Cumulative distributions of M_{DLS} for RC1 (blue) and RC2 (red) experiments

the distinct ADPR stacking pattern discussed above: the TST is characterized by retrogradational (R) stacking, with some aggradational (A) components in its oldest and youngest parts, the HST has aggradational-to-progradational (AP) stacking, the FSST is predominantly degradational (D), with a progradational (P) component during early stages, and the LST shows progradational-to-aggradational (PA) stacking. The thickness distribution of systems tracts varies considerably: the TST and FSST are on average much thicker than the LST and HST, as a result of the interaction between antecedent topography and the relative sea-level signal employed in the base-case simulation, which governs the spatio-temporal distribution of accommodation.

Post-processing of the net sediment accumulation records ($d(t_k)$) was used to extract preserved delta-lobe chronosomes by estimating net sediment accumulation rates over 1-kyr time intervals (Figure 7). The paleo-discharge network output was used accordingly to extract the dominant active channels throughout basin-fill evolution (Figure 8a,b). The extraction of the dominant channels allows us to detect the location of major avulsion sites (Figure 9a) and their distribution in the time-space (Wheeler) domain (Figure 9b). Figure 9b illustrates how the magnitude of a delta-lobe switch varies throughout the A/S cycle of the base case scenario. During early periods of relative sea-level fall only a few major avulsions occur in the vicinity of the sediment entry point. The frequency of major avulsions gradually diminishes during periods of fixed drainage when sea level drops below the shelf break. Base-level rise induces upstream aggradation which in turn increases avulsion frequency which peaks around the MFS, at the turnaround from retrogradation to progradation (TST to HST). The magnitude of delta-lobe switching is correlated with the location of major avulsion sites: proximal sites located close to the sediment entry point induce higher magnitudes of delta-lobe switching than distal sites.

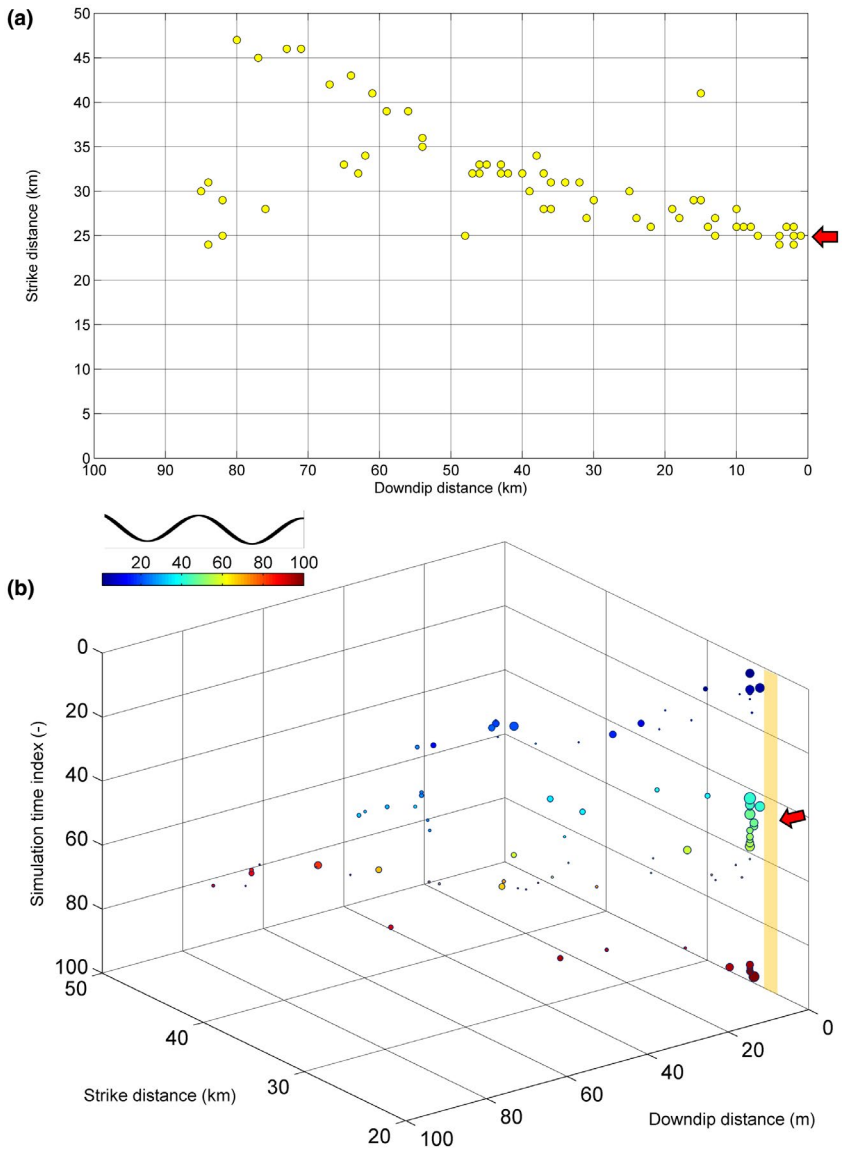

FIGURE 9 (a) Downdip and strike coordinates of major avulsion sites and (b) space-time (Wheeler) domain. The size of the dot marker is indicative of the size of the estimated M_{DLS} values for the base case scenario (RC1). The lower the simulation time index the younger the major avulsion. Red arrows indicate the location of the sediment entry point

4 | DISCUSSION

4.1 | Subdivision of the FSST

Previous outcrop- and seismic-based studies have illustrated the offlapping and downlapping of stratal packages interpreted to be the product of a descending shoreline trajectory during the late falling stage (Fielding, 2010, 2015; Li, Bhattacharya, & Zhu, 2011; Neal & Abreu, 2009; Plint & Nummedal, 2000; Zhu et al., 2012). Note numerical experiments show that there might be other formative mechanisms for these stratal packages (Zhang et al., 2019). Formation of the FSST occurs during the time interval marked by the BSFR and the surface corresponding to the lowest point on the relative sea-level curve (CC sensu Hunt & Tucker, 1992), and thus corresponds in duration to the maximum stratigraphic gap represented by the composite sequence boundary (Figure 6c). The abrupt decrease of major avulsions, which roughly coincides with the timing of shelf-break exposure, may be used to separate early from late FSST deposits (Figure 10b). All chronosomes that originated during the A/S cycle, with the exception of those formed during intervals in which sea-level drops below the shelf break, are mostly aggradational and may be subdivided into units bounded by delta-lobe abandonment surfaces associated with major avulsions (Figure 10b) (Dalman et al., 2015; Karamitopoulos et al., 2014). Owing to incision at the shelf edge and the near-absence of major avulsions, abandonment surfaces are not present in late FSST chronosomes, and their internal architecture is fundamentally different. Therefore, spatially distinct late FSST chronosomes that can be identified by the post-processing routines tend to have larger volumes, which is also expressed by their high degree of connectivity.

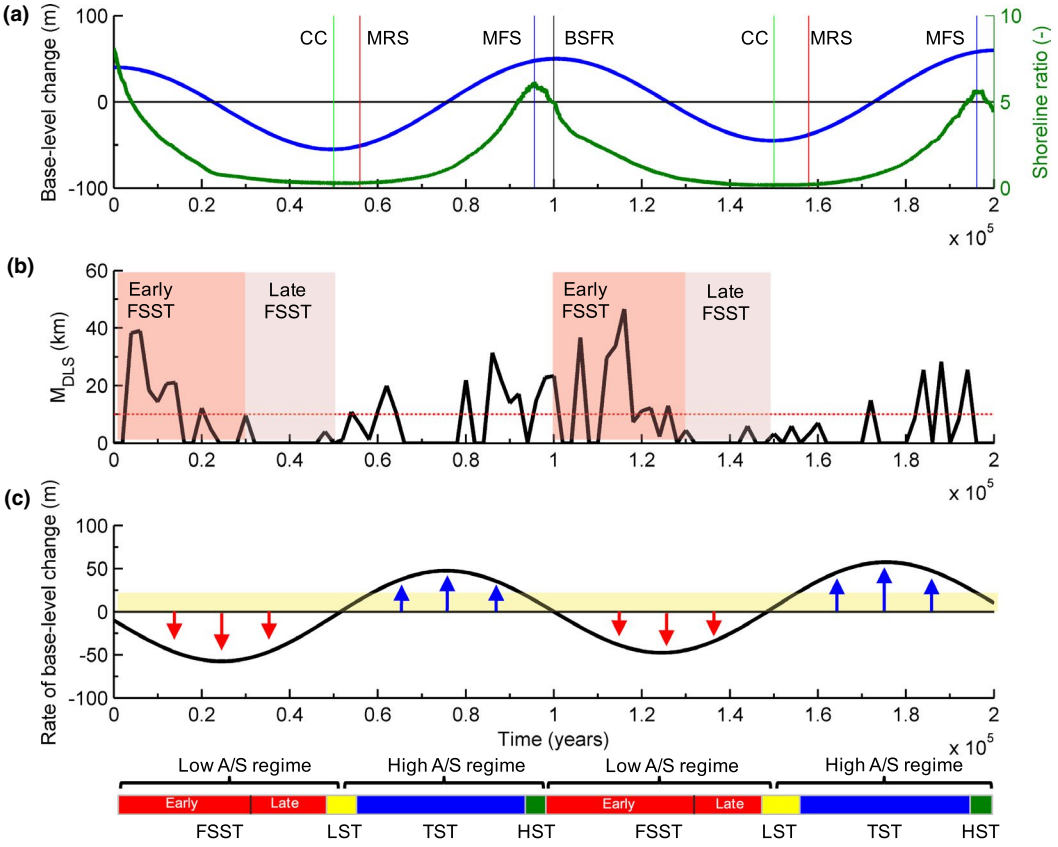

FIGURE 10 Sequence subdivision based on (a) normalized relative sea-level (blue) and shoreline ratio (green) curves. Correlative conformity (CC) (green lines) and basal surface of forced regression (BSFR) (black line) surfaces were picked at the lowest and highest points on the relative sea-level curve. Similarly, red and blue lines mark times of maximum regressive and maximum flooding surfaces corresponding to the lowest and highest points on the shoreline ratio curve. (b) Extracted major avulsion sites for the base case model. Timing and magnitude of M_{DLS} were used to differentiate between early and late falling stage systems tracts. Red dotted line corresponds to a threshold of 10 km along the coastline. (c) Rate of the relative sea-level curve and schematic sedimentation rate (yellow). Inflection points on the curve indicate the early and late stages of base-level rise (lowstand and highstand normal regressions, respectively). Overview of low-resolution and avulsion-based sequence subdivision is shown at the bottom (modified from Catuneanu et al., 2009)

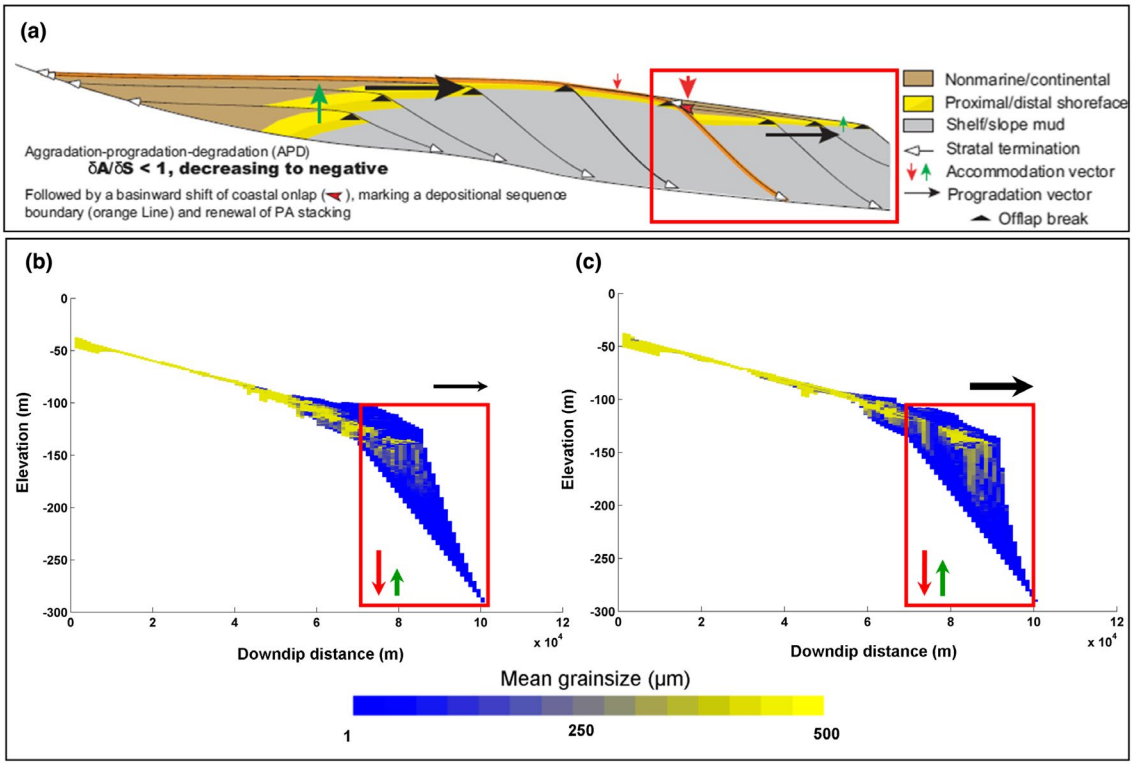

FIGURE 11 The late falling stage systems tract: (a) idealized stacking pattern associated with changing A/S ratio (modified from Neal & Abreu, 2009). (b) and (c) Longitudinal central sections at a strike distance of 25 km for scenarios RC3a and RC3b, respectively. Isolated sandy units encased by fine-grained sediments in RC3b form as a consequence of high-frequency relative sea-level oscillation

4.2 | *Icehouse* versus *Greenhouse stratigraphy*

The architecture of fluvial, delta-plain, and cross-shelf sedimentary segments is governed by the location of the river mouth and by the degree of shelf-break exposure. In the subaerial part of the system, the segments occupy the main pathways by which sediments are transferred from onshore to offshore areas. This is consistent with the previous field, experimental and numerical studies concerned with the origin, formation, and architectural arrangement of fluvial-shelf stratal units (Blum & Aslan, 2006; Blum & Hattier-Womack, 2009; Blum, Martin, Milliken, & Garvin, 2013; Holbrook, Scott, & Oboh-Ikuenobe, 2006; Martin et al., 2009; Pellegrini et al., 2017; Strong & Paola, 2008). High rates of base-level change as in the base case scenario (RC1), which represents icehouse periods, may expose the shelf-break during late FSST and initiate a phase of fixed and focused drainage marked by incision and lack of major avulsions (Figures 8a and 9b), dominated by mouth-bar induced bifurcations and high rates of progradation. The increased sediment discharge during the late falling stage in real-world systems caused by the merging of adjacent drainage areas (Blum et al., 2013) will increase the rate of progradation of late falling-stage chronosomes relative to our base-case scenario.

Conversely, low-amplitude sea-level change, representative of greenhouse periods (Figure 1a: green curve), prevents shelf-break emergence during the relative sea-level fall and hence the inherited topography (i.e., river and shelf gradients, shelf width) and the rate and amplitude of A/S variations regulate channel-network evolution. This morphodynamic pattern favours the residence of large sediment volumes along a limited shelf range (both at highstand and lowstand coastlines) which may be remobilized by coastal processes to give a massive accumulation of slope and basin-floor sediments (Blum & Hattier-Womack, 2009; Blum et al., 2013; Carvajal & Steel, 2006; Gong, Steel, Wang, Lin, & Olariu, 2016; Harris et al., 2020; Posamentier & Kolla, 2003; Ridente, 2016; Sømme, Helland-Hansen, Martinsen, & Thurmond, 2009; Steel, Olariu, Zhang, & Chen, 2019; Sweet & Blum, 2016). Major avulsions with relatively large river-mouth shifts dominate the entire sequence, in contrast with the icehouse pattern (Figure 8a,b). It is also clearly evident that the low-amplitude base-level changes increase the magnitude and frequency of delta-lobe switches (Figure 8b,c).

4.3 | High-frequency allogenic forcing

Figure 11b,c illustrates the longitudinal cross-sections of scenarios RC3a and RC3b, respectively, obtained without

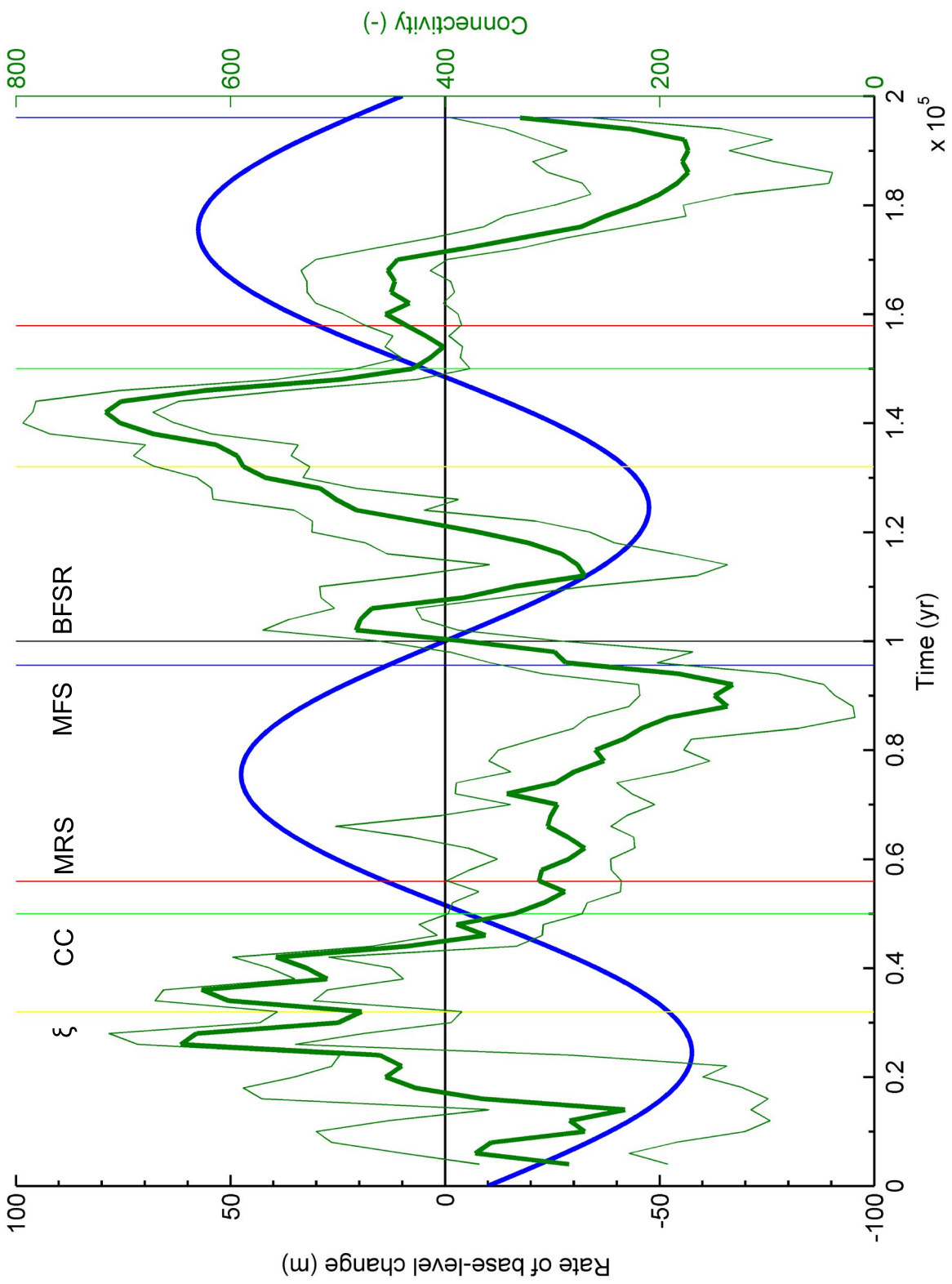

FIGURE 12 Median, P10 and P90 connectivity (green lines in the middle, lower and upper parts, respectively) and normalized rate of base-level change (blue) versus simulation time. Straight lines correspond to the classic isochronous sequence stratigraphic surfaces: correlative conformity (CC) (green lines), basal surface of forced regression (BSFR) (black lines), maximum regressive (MRS) (red lines), and maximum flooding surfaces (blue lines). The yellow lines (ξ) mark the periods of absence of major avulsions

and with a superimposed higher-frequency allogenic signal (25 kyr wavelength), respectively. As shown in Figure 11c, high-frequency allogenic forcing may cause landward and basinward fluctuation of the mouth bar and shoreline areas, which severs the connection between the fluvial distributary segment and the area beyond the shelf break, causing fragmentation of the coarse-grained units. This is consistent with previous experimental work on coastal-plain and cross-shelf paleovalley formation in response to high-frequency sea-level change which demonstrated a disequilibrium response to external forcing (Strong & Paola, 2008). From a sequence-stratigraphic perspective, the result of such high-frequency fluctuations has been previously described as a "stranded parasequence" (Plint & Nummedal, 2000) and/or high-frequency cut and fill cycle (Zhu et al., 2012). Our simulations suggest that such "stranded" units may represent short episodes of stagnant or rising base level during an overall base-level fall.

4.4 | Large-scale connectivity

Figure 12 illustrates how large-scale connectivity varies throughout the base case scenario. The earliest and late FSST chronosomes demonstrate the highest large-scale connectivity in their proximal and distal areas, respectively. Avulsion frequency increases during the periods of relative sea-level rise as a consequence of the combined effect of auto- and allogenic aggradation, which in turn decreases large-scale connectivity. LST and early TST chronosomes demonstrate moderate connectivity which is amplified in the vicinity of the shelf break owing to higher back-fill rates in the major trunk channel and the adjacent topographic lows.

5 | CONCLUSIONS

In this paper, we used a process-based stratigraphic model of fluvio-deltaic stratigraphy to simulate fluvio-deltaic system evolution by simulating accommodation-to-sediment-supply (A/S) cycles of varying wavelength and amplitude. A number of post-processing routines were developed to investigate channel-network evolution throughout the A/S cycles, estimate net sediment accumulation rates and extract chronostratigraphically constrained lithosomes (or chronosomes). As shown in Figure 12, post-processing provides a straightforward measure of large-scale connectivity, that is, the spatial distribution of high net-gross lithologies. Our approach permits the quantification of sub-seismic-scale sedimentary heterogeneity of fluvio-deltaic deposits and provides a coherent predictive model of lithofacies distribution throughout the modelled A/S cycles. The earliest and late FSST chronosomes demonstrate the highest large-scale connectivity in their proximal and distal areas, respectively. LST and early TST chronosomes demonstrate moderate connectivity which is amplified in the vicinity of the shelf break owing to higher back-fill rates in the major trunk channel and the adjacent topographic lows. The magnitude and frequency of delta-lobe switches vary throughout the A/S cycle. The stratigraphic expression of a delta-lobe switch marked by a major avulsion provides the key to a high-resolution subdivision of fluvio-deltaic deposits into chronosomes. The timing of avulsion-induced abandonment surfaces in real-world stratigraphy will most likely be influenced by the intertwined perturbations of high-frequency allogenic forcing and differential subsidence. Sedimentary packages of the late FSST form in response to the exposure of the shelf edge at the terminal parts of the incised-valley transfer system, and become physically isolated to form "stranded" segments. The architectural arrangement of these late FSST chronosomes, which develop during periods of sporadic major avulsions, is fundamentally different from that of the other chronosomes, which develop under the conditions of (local) aggradation by means of rapid avulsion-induced depocentre shifts. High-frequency allogenic forcing may cause the landward and basinward fluctuation of the mouth bar and shoreline areas and interrupt the connection between the fluvial distributary segment leading to "stranded" coarse-grained segments.

5.1 | Future research

The results of this study suggest that subsurface lithology prediction at sub-seismic scales may strongly benefit from the analysis of synthetic 3-D stratigraphic records generated with process-based numerical models that account for allogenic and autogenic forcing. The predictive capabilities of process-based stratigraphic models may be improved by (1) expanding the experimental parameter space and using the proposed post-processing routines to expand on the generic lessons learned in this study and (2) directly matching to real-world settings by linking surface processes to substrate characteristics (e.g., groundwater table fluctuation and subsidence) as well as by integrating multiscale, multitype datasets (including satellite and geophysical/geological data supported by absolute and relative dating techniques) in order to approximate the initial and boundary conditions of prospective sedimentary basins; thus more accurately reconstruct the genetic structure and physical continuity of fluvio-deltaic chronosomes.

The former approach may be used in settings were data density is limited, the latter in settings were enough knowledge is present to allow a reasonable estimate of the necessary model parameters to obtain a good fit.

ACKNOWLEDGEMENTS

Perceptive reviews by Jinyu Zhang, Tore Grane Klausen, and an anonymous reviewer have been very helpful in shaping the paper. We acknowledge constructive and helpful comments on earlier versions of the manuscript by Zoltan Sylvester, Joshua Dixon, Jory Pacht, Allard Martinius, Gary Hampson, and Geert de Bruin. We would also like to thank Editor-in-Chief Atle Rotevatn and Associate Editor Peter Burgess for the excellent handling of the manuscript.

DATA AVAILABILITY STATEMENT

The data that support the findings of this study are available from the corresponding author upon reasonable request.

ORCID

Pantelis Karamitopoulos https://orcid.org/0000-0001-8121-7487

REFERENCES

Allen, G., Lang, S., Musakti, O., & Chirinos, A. (1996). Application of sequence stratigraphy to continental successions. In *Implications for Mesozoic cratonic interior basins of Eastern Australia*. Mesozoic Geology of the Eastern Australian Plate Conference, Brisbane, Australia, Extended Abstracts, 22–26.

Allen, P. A., & Allen, J. R. (2013). *Basin analysis: Principles and application to petroleum play* assessment (version 3rd ed., 632 pp.). Chichester, UK: Wiley-Blackwell.

Barrell, J. (1917). Rhythms and the measurement of geologic time. *Geological Society of America Bulletin*, *28*, 745–904.

Bhattacharya, J. P. (2011). Practical problems in the application of the sequence stratigraphic method and key surfaces: Integrating observations from ancient fluvial–deltaic wedges with Quaternary and modelling studies. *Sedimentology*, *58*, 120–169. https://doi.org/10.1111/j.1365-3091.2010.01205.x

Blum, M. D., & Aslan, A. (2006). Signatures of climate vs. sea- level change within incised valley-fill successions: Quaternary examples from the Texas Gulf Coast. *Sedimentary Geology*, *190*, 177–211. https://doi.org/10.1016/j.sedgeo.2006.05.024

Blum, M. D., & Hattier-Womack, J. (2009). Climate change, sea-level change, and fluvial sediment supply to deepwater systems. In B. Kneller, O. J. Martinsen, & B. McCaffrey (Eds.), *External controls on deep water depositional systems: Climate, sea-level, and sediment flux*. SEPM Special Publication. *92*, 15–39.

Blum, M. D., Martin, B. J., Milliken, K., & Garvin, M. (2013). Paleovalley systems: Insights from quaternary analogs and experiments. *Earth-Science Reviews*, *116*, 128–169. https://doi.org/10.1016/j.earscirev.2012.09.003

Burgess, P. M. (2012). A brief review of developments in stratigraphic forward modelling 2000–2009. In D. G. Roberts, & A. W. Bally (Eds.), *Regional geology and tectonics: Principles of geologic analysis* (pp. 378–404). Amsterdam: Elsevier.

Burgess, P. M. (2016). The future of the sequence stratigraphy paradigm: Dealing with a variable third dimension. *Geology*, *44*, 335–336.

Burgess, P. M., Allen, P. A., & Steel, R. J. (2016). Introduction to the future of sequence stratigraphy: Evolution or revolution? *Journal of the Geological Society*, *173*, 801–802. https://doi.org/10.1144/jgs2016-078

Burgess, P. M., Lammers, H. M., Van Oosterhout, C., & Granjeon, D. (2006). Multivariate sequence stratigraphy: Tackling complexity and uncertainty with stratigraphic forward modeling, multiple scenarios and conditional frequency maps. *AAPG Bulletin*, *90*, 1883–1901.

Burgess, P. M., & Prince, G. D. (2015). Non-unique stratal geometries: Implications for sequence stratigraphic interpretations. *Basin Research*, *27*, 352–365. https://doi.org/10.1111/bre.12082

Carvajal, C., & Steel, R. (2006). Thick turbidite successions from supply-dominated shelves during sea-level highstand. *Geology*, *34*, 665–668. https://doi.org/10.1130/G22505.1

Catuneanu, O. (2020). Sequence stratigraphy in the context of the 'modeling revolution'. *Marine and Petroleum Geology*, *116*, 104309. https://doi.org/10.1016/j.marpetgeo.2020.104309

Catuneanu, O., Abreu, V., Bhattacharya, J. P., Blum, M. D., Dalrymple, R. W., Eriksson, P. G., … Winker, C. (2009). Towards the standardization of sequence stratigraphy. *Earth-Science Reviews*, *92*, 1–33. https://doi.org/10.1016/j.earscirev.2008.10.003

Catuneanu, O., Galloway, W. E., Kendall, C. G., St, C., Miall, A. D., Posamentier, H. W., … Tucker, M. E. (2011). Sequence stratigraphy: Methodology and nomenclature. *Newsletter on Stratigraphy*, *44*, 173–245. https://doi.org/10.1127/0078-0421/2011/0011

Charvin, K., Gallagher, K. L., Hampson, G., & Labourdette, R. (2009). A Bayesian approach to inverse modelling of stratigraphy, part I: Method. *Basin Research*, *21*, 5–25.

Cross, T. A. (1990). *Quantitative dynamic stratigraphy* (625 p.). Upper Saddle River, NJ: Prentice Hall.

Cross, T., & Lessenger, M. (1999). Construction and application of stratigraphic inverse model. In: J. W. Harbaugh et al. (Eds.), *Numerical experiments in stratigraphy: Recent advances in stratigraphic and sedimentologic computer simulations*. SEPM Special Publication, *62*, 69–83.

Dalman, R. A. F., & Weltje, G. J. (2008). Sub-grid parameterisation of fluvio-deltaic processes and architecture in a basin-scale stratigraphic model. *Computers & Geosciences*, *34*, 1370–1380. https://doi.org/10.1016/j.cageo.2008.02.005

Dalman, R. A. F., & Weltje, G. J. (2012). SimClast: An aggregated forward stratigraphic model of continental shelves. *Computers & Geosciences*, *38*, 115–126. https://doi.org/10.1016/j.cageo.2011.05.014

Dalman, R. A. F., Weltje, G. J., & Karamitopoulos, P. (2015). High-resolution sequence stratigraphy of fluvio–deltaic systems: Prospects of system-wide chronostratigraphic correlation. *Earth and Planetary Science Letters*, *412*, 10–17. https://doi.org/10.1016/j.epsl.2014.12.030

Embry, A. F. (1995). Sequence boundaries and sequence hierarchies: problems and proposals. In R. J. Steel, V. L. Felt, E. P. Johannessen, & C. Mathieu (Eds.), *Sequence stratigraphy on the Northwest European Margin*. Norwegian Petroleum Society Special Publication *5*, 1–11.

Emery, D., & Myers, K. J. (1996). *Sequence stratigraphy* (297 p.). Oxford, UK: Blackwell.

Falivene, O., Frascati, A., Gesbert, S., Pickens, J., Hsu, Y., & Rovira, A. (2014). Automatic calibration of stratigraphic forward models for predicting reservoir presence in exploration. *AAPG Bulletin*, *98*, 1811–1835.

Feynman, R. P. (1982). Simulating physics with computers. *International Journal of Theoretical Physics*, *21*, 467–488. https://doi.org/10.1007/BF02650179

Fielding, C. R. (2010). Planform and facies variability in asymmetric deltas: Facies analysis and depositional architecture of the Turonian

Ferron sandstone in the Western Henry mountains, south-central Utah, USA. *Journal of Sedimentary Research*, *80*, 455–479. https://doi.org/10.2110/jsr.2010.047

Fielding, C. R. (2015). Anatomy of falling-stage deltas in the Turonian Ferron sandstone of the western Henry mountains syncline, Utah: Growth faults, slope failures and mass transport complexes. *Sedimentology*, *62*, 1–26. https://doi.org/10.1111/sed.12136

Frazier, D. E. (1974). Depositional episodes: their relationship to the Quaternary stratigraphic framework in the northwestern portion of the Gulf basin, Austin, Texas, Bureau of Economic Geology, Geologic Circular 74-1, 28 p.

Galloway, W. E. (1975). Process framework for describing the morphologic and stratigraphic evolution of deltaic depositional systems. In M. L. Broussard (Ed.), *Deltas, models for exploration* (pp. 87–98). Houston, TX: Houston Geological Society.

Galloway, W. E. (1989). Genetic stratigraphic sequences in basin analysis. I. Architecture and genesis of flooding-surface bounded depositional units. *AAPG Bulletin*, *73*, 125–142.

Gong, C., Steel, R. J., Wang, Y., Lin, C., & Olariu, C. (2016). Shelf-margin architecture variability and its role in sediment-budget partitioning into deep-water areas. *Earth-Science Reviews*, *154*, 72–101. https://doi.org/10.1016/j.earscirev.2015.12.003

Granjeon, D. (2014). 3D forward modelling of the impact of sediment transport and base level cycles on continental margins and incised valleys. *International Association Sedimentology Special Publication*, *46*, 453–472.

Granjeon, D., & Joseph, P. (1999). Concepts and applications of a 3D multiple lithology, diffusive model in stratigraphic modelling. In J. W. Harbaugh, W. L. Watney, E. Rankey, R. L. Slingerland, R. Golstein, & E. K. Franseen (Eds.), *Numerical experiments in stratigraphy: Recent advances in stratigraphic and sedimentologic computer simulations*. SEPM Special Publication, *62*, 197–210.

Griffiths, C. M. (1996). A stratigraphy for the 21st Century. *First Break*, *14*, 383–389. https://doi.org/10.3997/1365-2397.1996020

Griffiths, C. M., & Nordlund, U. (1993). Chronosome and quantitative stratigraphy. *Geoinformatics*, *4*, 327–336.

Hajek, E. A., & Wolinsky, M. A. (2012). Simplified process modeling of river avulsion and alluvial architecture: Connecting models and field data. *Sedimentary Geology*, *257–260*, 1–30. https://doi.org/10.1016/j.sedgeo.2011.09.005

Hampson, G. J. (2016). Towards a sequence stratigraphic solution set for autogenic processes and allogenic controls: Upper Cretaceous strata, Book Cliffs, Utah, USA. *Journal of the Geological Society*, *173*, 817–836. https://doi.org/10.1144/jgs2015-136

Harris, A. D., Covault, J. A., Baumgardner, S., Sun, T., & Granjeon, D. (2020). Numerical modeling of icehouse and greenhouse sea-level changes on a continental margin: Sea-level modulation of deltaic avulsion processes. *Marine and Petroleum Geology*, *111*, 807–814. https://doi.org/10.1016/j.marpetgeo.2019.08.055

Helland-Hansen, W., & Hampson, G. J. (2009). Trajectory analysis: Concepts and applications. *Basin Research*, *21*, 454–483. https://doi.org/10.1111/j.1365-2117.2009.00425.x

Helland-Hansen, W., & Martinsen, O. J. (1996). Shoreline trajectories and sequences: description of variable depositional-dip scenarios. *Journal of Sedimentary Research*, *66*, 1670–1688.

Holbrook, J., & Bhattacharya, J. P. (2012). Reappraisal of the sequence boundary in time and space: Case and considerations for an SU (subaerial unconformity) that is not a sediment bypass surface, a time barrier, or an unconformity. *Earth-Science Reviews*, *113*, 271–302. https://doi.org/10.1016/j.earscirev.2012.03.006

Holbrook, J. M., Scott, R. W., & Oboh-Ikuenobe, F. E. (2006). Base-level buffers and buttresses: A model for upstream verses downstream control on preservation of fluvial geometry and architecture within sequences. *Journal of Sedimentary Research*, *76*, 162–174.

Hunt, D., & Tucker, M. E. (1992). Stranded parasequences and the forced regressive wedge systems tract: Deposition during base-level fall. *Sedimentary Geology*, *81*, 1–9. https://doi.org/10.1016/0037-0738(92)90052-S

Imhof, M., & Sharma, A. K. (2006). Quantitative seismostratigraphic inversion of a prograding delta from seismic data. *Marine and Petroleum Geology*, *23*, 735–744.

Jervey, M. T. (1988). Quantitative geological modeling of siliciclastic rock sequences and their seismic expression. In C. K. Wilgus, B. S. Hastings, C. G. S. C. Kendall, H. W. Posamentier, C. A. Ross, & J. C. Van Wagoner (Eds.), *Sea-level changes: An integrated approach*. SEPM Special Publication. *42*, 47–69.

Karamitopoulos, P., Weltje, G. J., & Dalman, R. A. F. (2014). Allogenic controls on autogenic variability in fluvio-deltaic systems: Inferences from analysis of synthetic stratigraphy. *Basin Research*, *26*, 767–779. https://doi.org/10.1111/bre.12065

Karssenberg, D. J., & Törnqvist, T. E., & Bridge, J. S. (2001). Conditioning a process-based model of sedimentary architecture to well data. *Journal of Sedimentary Research*, *71*, 868–879.

Karssenberg, D. J., De Vries, M., & Bridge, J. S. (2007). *Conditioning a process-based fluvial-stratigraphy model to well data by inverse estimation of model inputs using a genetic algorithm. AAPG Search and Discovery Article #90063*. Long Beach, CA: AAPG Annual Convention.

Li, W., Bhattacharya, J. P., & Zhu, Y. (2011). Architecture of a forced regressive systems tract in a Turonian Ferron "Notom Delta", southern Utah, U.S.A. *Marine and Petroleum Geology*, *28*, 1517–1529.

Madof, A. S., Harris, A. D., & Connell, S. D. (2016). Nearshore along-strike variability: Is the concept of the systems tract unhinged? *Geology*, *44*, 315–318. https://doi.org/10.1130/G37613.1

Martin, J., Paola, C., Abreu, V., Neal, J., & Sheets, B. (2009). Sequence stratigraphy of experimental strata under known conditions of differential subsidence and variable base level. *AAPG Bulletin*, *93*, 503–533. https://doi.org/10.1306/12110808057

Martinez, P. A., & Harbaugh, J. W. (1993). *Simulating nearshore environments*. Oxford, UK: Pergamon Press.

Martinius, A. W., Elfenbein, C., & Keogh, K. J. (2014). Applying accommodation versus sediment supply ratio concepts to stratigraphic analysis and zonation of a fluvial reservoir. *International Association of Sedimentologists, Special Publication*, *46*, 101–126.

Martinsen, O. J., Ryseth, A., Helland-Hansen, W., Flesche, H., Torkildsen, G., & Idil, S. (1999). Stratigraphic base level and fluvial architecture: Ericson Sandstone (Campanian), Rock Springs Uplift, SW Wyoming, USA. *Sedimentology*, *46*, 235–259. https://doi.org/10.1046/j.1365-3091.1999.00208.x

Matthews, R. K. (1974). *Dynamic stratigraphy* (370 p.). Upper Saddle River, NJ: Prentice Hall.

Meijer, X. D. (2002). Modelling the drainage evolution of a river-shelf system forced by Quaternary glacio-eustasy. *Basin Research*, *14*, 361–377. https://doi.org/10.1046/j.1365-2117.2002.00187.x

Miall, A. D. (2010). *The geology of stratigraphic sequences*, 2nd edn (316 p.). Berlin: Springer-Verlag.

Miall, A. D. (2014). Updating uniformitarianism: stratigraphy as just a set of 'frozen accidents'. In D. G. Smith, R. J. Bailey, P. M. Burgess,

& A. J. Fraser (Eds.), *Strata and time: Probing the gaps in our understanding* (Vol. *404*, pp. 11–36). London, UK: Geological Society, Special Publications.

Miller, K. G., Kominz, M. A., Browning, J. V., Wright, J. D., Mountain, G. S., Katz, M. E., … Pekar, S. F. (2005). The Phanerozoic record of global sea-level change. *Science*, *310*, 1293–1298. https://doi.org/10.1126/science.1116412

Mitchum Jr., R. M., Vail, P. R., & Thompson, S., III. (1977). Seismic stratigraphy and global changes of sea level, Part 2, The depositional sequence as a basic unit for stratigraphic analysis. In C. E. Payton (Ed.), *Seismic stratigraphy—applications to hydrocarbon exploration*. American Association of Petroleum Geologists Memoir. *26*, 53–62).

Muto, T., & Steel, R. J. (1997). Principles of regression and transgression: The nature of the interplay between accommodation and sediment supply. *Journal of Sedimentary Research*, *67*, 994–1000. https://doi.org/10.1306/D42686A8-2B26-11D7-8648000102C1865D

Muto, T., & Steel, R. J. (2002). Role of autoretreat and A/S changes in the understanding of deltaic shoreline trajectory: A semi-quantitative approach. *Basin Research*, *14*, 303–318. https://doi.org/10.1046/j.1365-2117.2002.00179.x

Muto, T., & Steel, R. J. (2004). Autogenic response of fluvial deltas to steady sea-level fall: Implications from flume-tank experiments. *Geology*, *32*, 401–404. https://doi.org/10.1130/G20269.1

Muto, T., Steel, R. J., & Burgess, P. M. (2016). Contributions to sequence stratigraphy from analogue and numerical experiments. *Journal of the Geological Society*, *173*, 837–844. https://doi.org/10.1144/jgs2015-127

Neal, J., & Abreu, V. (2009). Sequence stratigraphy hierarchy and the accommodation succession method. *Geology*, *37*, 779–782. https://doi.org/10.1130/G25722A.1

Paola, C. (2000). Quantitative models of sedimentary basin filling. *Sedimentology*, *47*, 121–178.

Paola, C., Heller, P. L., & Angevine, C. L. (1992). The large-scale dynamics of grain size variation in alluvial basins, 1: Theory. *Basin Research*, *4*, 73–90. https://doi.org/10.1111/j.1365-2117.1992.tb00145.x

Paola, C., Straub, K. M., Mohrig, D. C., & Reinhardt, L. (2009). The "unreasonable effectiveness" of stratigraphic and geomorphic experiments. *Earth Science Reviews*, *97*, 1–43. https://doi.org/10.1016/j.earscirev.2009.05.003

Payton, C. E. (1977). Seismic stratigraphy—Applications to the exploration of sedimentary basins. *AAPG Memoir*, *26*, 516 p.

Pellegrini, C., Maselli, V., Gamberi, F., Asioli, A., Bohacs, K. M., Drexler, T. M., & Trincardi, F. (2017). How to make a 350-m-thick lowstand systems tract in 17,000 years: The Late Pleistocene Po River (Italy) lowstand wedge. *Geology*, *45*, 327–330. https://doi.org/10.1130/G38848.1

Pellegrini, C., Patruno, S., Helland-Hansen, W., Steel, R. J., & Trincardi, F. (2020). Clinoforms and clinothems: Fundamental elements of basin infill. *Basin Research*, *32*, 187–205. https://doi.org/10.1111/bre.12446

Plint, A. G., & Nummedal, D. (2000). The falling stage systems tract: Recognition and importance in sequence stratigraphic analysis. In D. Hunt & R. L. Gawthorpe (Eds.), *Sedimentary response to forced regression* (Vol. *172*, pp. 1–17). London, UK: Geological Society, Special Publications.

Plotnick, R. (1986). A fractal model for the distribution of stratigraphic hiatuses. *Journal of Geology*, *94*, 885–890. https://doi.org/10.1086/629094

Posamentier, H. W., & Allen, G. P. (1999). *Siliciclastic sequence stratigraphy-concepts and applications*. Soc. Econ. Paleo. and Mineral. (SEPM) Concepts in Sedimentology and Paleontology, *7*, 210 p.

Posamentier, H. W., Jervey, M. T., & Vail, P. R. (1988). Eustatic controls on clastic deposition. I. Conceptual framework. In C. K. Wilgus, B. S. Hastings, C. G. S. C. Kendall, H. W. Posamentier, C. A. Ross, & J. C. Van Wagoner (Eds.), *Sea level changes—An integrated approach*. SEPM Special Publication. *42*, 110–124.

Posamentier, H. W., & Kolla, V. (2003). Seismic geomorphology and stratigraphy of depositional elements in deep-water settings. *Journal of Sedimentary Research*, *73*, 367–388. https://doi.org/10.1306/111302730367

Posamentier, H. W., & Vail, P. R. (1988). Eustatic controls on clastic deposition. II. Sequence and systems tract models. In C. K. Wilgus, B. S. Hastings, C. G. S. C. Kendall, H. W. Posamentier, C. A. Ross, & J. C. Van Wagoner (Eds.), *Sea level changes—An integrated approach*. SEPM Special Publication. *42*, 125–154.

Ridente, D. (2016). Releasing the sequence stratigraphy paradigm: Overview and perspectives. *Journal of the Geological Society*, *173*, 845–853. https://doi.org/10.1144/jgs2015-140

Ritchie, B. D., Gawthorpe, R. L., & Hardy, S. (2004a). Three-dimensional numerical modelling of deltaic depositional sequences 1: Influence of the rate and magnitude of sea-level change. *Journal of Sedimentary Research*, *74*, 203–220.

Ritchie, B. D., Gawthorpe, R. L., & Hardy, S. (2004b). Three-dimensional numerical modelling of deltaic depositional sequences 2: Influences of local controls. *Journal of Sedimentary Research*, *74*, 221–238.

Sadler, P. M. (1981). Sediment accumulation rates and the completeness of stratigraphic sections. *Journal of Geology*, *89*, 569–584. https://doi.org/10.1086/628623

Sadler, P. M., & Strauss, D. J. (1990). Estimation of completeness of stratigraphical sections using empirical data and theoretical models. *Journal of the Geological Society*, *147*, 471–485. https://doi.org/10.1144/gsjgs.147.3.0471

Schlager, W. (1993). Accommodation and supply—A dual control on stratigraphic sequences. *Sedimentary Geology*, *86*, 111–136. https://doi.org/10.1016/0037-0738(93)90136-S

Schultz, E. H. (1982). The chronosome and supersome: Terms proposed for low-rank chronostratigraphic units. *Bulletin of Canadian Petroleum Geology*, *30*, 29–33.

Shanley, K. W., & McCabe, P. J. (1993). Alluvial architecture in a sequence stratigraphic framework: A case history from the Upper Cretaceous of southern Utah, USA. In S. S. Flint & I. D. Bryant (Eds.), *The geological modelling of hydrocarbon reservoirs and outcrop analogues*. International Association of Sedimentologists, Special Publication. *15*, 21–56.

Sheets, B., Hickson, T. A., & Paola, C. (2002). Assembling the stratigraphic record: Depositional patterns and time-scales in an experimental alluvial basin. *Basin Research*, *14*, 287–301. https://doi.org/10.1046/j.1365-2117.2002.00185.x

Sømme, T. O., Helland-Hansen, W., Martinsen, O. J., & Thurmond, J. B. (2009). Relationships between morphological and sedimentological parameters in source-to-sink systems: a basis for predicting semi-quantitative characteristics in subsurface systems. *Basin Research*, *21*, 361–387.

Steel, R. J., Olariu, C., Zhang, J., & Chen, S. (2019). What is the topset of a shelf-margin prism? *Basin Research*, *32*, 263–278. https://doi.org/10.1111/bre.12394

Strong, N., & Paola, C. (2008). Valleys that never were: Time surfaces versus stratigraphic surfaces. *Journal of Sedimentary Research*, *78*, 579–593. https://doi.org/10.2110/jsr.2008.059

Sweet, M. L., & Blum, M. D. (2016). Connections between fluvial to shallow marine environments and submarine canyons: Implications for sediment transfer to deep water. *Journal of Sedimentary Research*, *86*, 1147–1162. https://doi.org/10.2110/jsr.2016.64

Swift, D. J. P., & Thorne, J. A. (1991). Sedimentation on continental margins, I: a general model for shelf sedimentation. In D. J. P. Swift, G. F. Oertel, R. W. Tillman, & J. A. Thorne (Eds.), *Shelf sand and sandstone bodies*. International Association of Sedimentologists, Special Publication. *14*, 3–31.

Tetzlaff, D. M., & Harbaugh, J. W. (1989). *Simulating clastic sedimentation: Computer methods in the geosciences* (p. 202). New York, NY: Van Nostrand Reinhold.

Thorne, J. A., & Swift, D. J. P. (1991). Sedimentation on continental margins, II: application of the regime concept. In D. J. P. Swift, G. F. Oertel, R. W. Tillman, & J. A. Thorne (Eds.), *Shelf sand and sandstone bodies: geometry, facies and sequence stratigraphy*. International Association of Sedimentologists, Special Publication. *14*, 33–58.

Tipper, J. C. (2000). Patterns of stratigraphic cyclicity. *Journal of Sedimentary Research*, *70*, 1262–1279. https://doi.org/10.1306/031700701262

Tipper, J. C. (2015). The importance of doing nothing: stasis in sedimentation systems and its stratigraphic effects. In D. G. Smith, R. J. Bailey, P. M. Burgess, & A. J. Fraser (Eds.), *Strata and time: Probing the gaps in our understanding* (Vol. *404*, pp. 105–122). London, UK: Geological Society, Special Publications.

Tipper, J. C. (2016). Measured rates of sedimentation: What exactly are we estimating, and why? *Sedimentary Geology*, *339*, 151–171. https://doi.org/10.1016/j.sedgeo.2016.04.003

Vail, P. R. (1987). Seismic stratigraphy interpretation using sequence stratigraphy, Part 1: seismic stratigraphy interpretation procedure. In: A.W. Bally (Eds.), *Atlas of Seismic Stratigraphy*. Am. Assoc. Pet. Geol. Stud. Geol., *27*, 1–10.

Vail, P. R., Mitchum, R. M., & Thompson, S., III. (1977). Seismic stratigraphy and global changes of sea level; Part 4, Global cycles of relative changes of sea level. In C. E. Payton (Ed.), *Seismic stratigraphy; applications to hydrocarbon exploration*. AAPG Memoir. *26*, 83–97.

Von Neumann, J. (1966). *Theory of self reproducing automata* (418 p.). University of Illinois Press.

Weltje, G. J., & Roberson, S. (2012). Numerical methods for integrating particle-size frequency distributions. *Computers & Geosciences*, *44*, 156–167. https://doi.org/10.1016/j.cageo.2011.09.020

Wijns, C., Poulet, T., Boschetti, F., Dyt, C., & Griffiths, C. M. (2004). Interactive inverse methodology applied to stratigraphic forward modelling. In: A. Curtis & R. Wood (Eds.), *Geological prior information: Informing science and engineering*. Geological Society of London Special Publications, *239*, 147–155.

Wolfram, S. (2002). *A new kind of science* (1197 p.). Champaign, IL: Wolfram Media.

Wright, V. P., & Marriott, S. B. (1993). The sequence stratigraphy of fluvial depositional systems: The role of floodplain sediment storage. *Sedimentary Geology*, *86*, 203–210. https://doi.org/10.1016/0037-0738(93)90022-W

Zhang, J., Burgess, P. M., Granjeon, D., & Steel, R. (2019). Can sediment supply variations create sequences? Insights from stratigraphic forward modelling. *Basin Research*, *31*, 274–289. https://doi.org/10.1111/bre.12320

Zhu, Y., Bhattacharya, J. P., Li, W., Lapen, T. J., Jicha, B. R., & Singer, B. S. (2012). Milankovitch-scale sequence stratigraphy and stepped forced regressions of the Turonian Ferron Notom Deltaic Complex, South-central Utah, U.S.A. *Journal of Sedimentary Research*, *82*, 723–746. https://doi.org/10.2110/jsr.2012.63

How to cite this article: KaramitopoulosP, Weltje GJ, Dalman RAF. Large-scale connectivity of fluvio-deltaic stratigraphy: Inferences from simulated accommodation-to-supply cycles and automated extraction of chronosomes. *Basin Res*. 2021;33:382–402. https://doi.org/10.1111/bre.12471

APPENDIX A

Post-processing routines

Constrained cubic spline interpolation

The depositional output for every grid cell was stored as stratigraphic thickness D (cumulative net sediment accumulation) versus simulation time records (Figure A1a). The constrained cubic spline interpolation method (Weltje & Roberson, 2012) was used to generate a smooth continuous record of cumulative thickness values. The method provides an explicit first derivative at every point and ensures the smooth curve characteristics of linear interpolation while preventing the oscillatory (overshooting) behaviour of cubic splines (Runge's phenomenon).

Net sediment accumulation rate

The interpolation method was applied in order to approximate point-support rates (R) over a specified time interval (Tipper, 2016). Net sediment accumulation rate is estimated using a central difference operator of the cumulative net sediment accumulation function:

$$R_{s_i t_i} = \delta D_{s_i,t_i} = \delta D_{s_i,t_{i+\frac{1}{2}}} - \delta D_{s_i,t_{i-\frac{1}{2}}},$$

where s and t are the space and time coordinates. The central difference instead of forward or backward operators was deployed in order to minimize the expected truncation error (Figure A1a). Net sediment accumulation rates were estimated over kyr time-scale intervals which were assumed to be sufficient time for sites to receive the amount of sediment necessary to form distinct delta-lobe units (Figure A1b).

Delta-lobe initialization by binary transformation

The binary transformation (or thresholding) algorithm operates on the generated cumulative distribution of net deposition

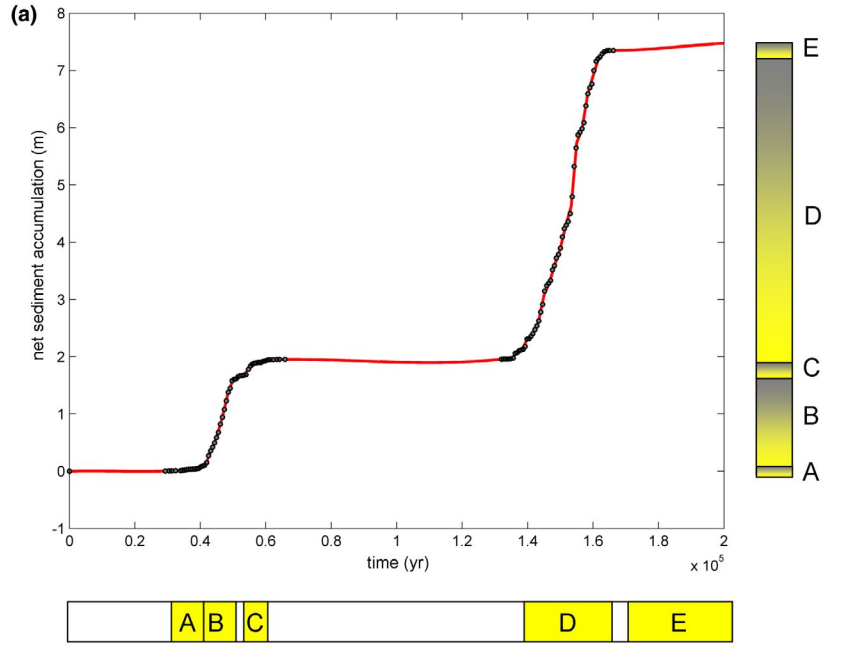

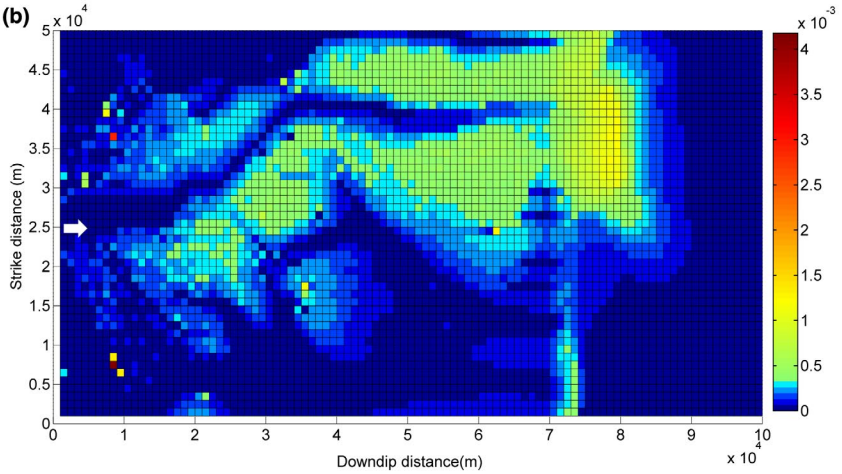

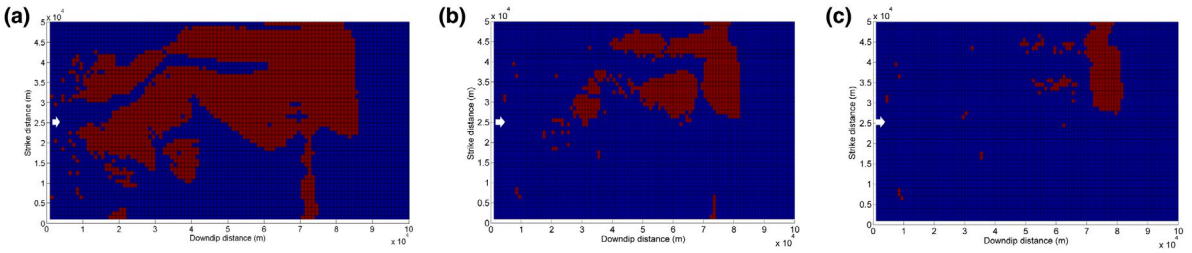

FIGURE A1 (a) Stratigraphic thickness (cumulative net sediment accumulation) versus simulation time for random grid cell. Fitted constrained cubic spline (red curve) used for interpolation between data points. Plateaus in the graph correspond to periods of stasis (bypass or non-deposition). Graph viewed as Cantor function below (modified after Plotnick, 1986, Figure 5). (b) Example of estimated net sediment accumulation rates (m/yr) during relative sea-level fall at ~20 kyr. White arrow indicates the location of the sediment entry point

FIGURE A2 Net delta-lobe facies (red) extracted based on 60% (a), 80% (b), and 90% (c) of the overall sample population on the net sediment accumulation rate cumulative histogram. White arrows indicate the location of the sediment entry point

rates and aims to capture genetic delta-lobe units characterized by high net deposition rates. The assigned cut-off values correspond to the selected threshold population percentage of net sediment accumulation rates (Figure A2). The P10 point (90% of the overall population) is the value for which 10% of the data points are higher. We assumed in this case that the P10 curve was an acceptable prediction. After the binary transformation operation, the values below the threshold were nullified and therefore assigned as "unpopulated" while the ones above became equal to 1 ("populated").

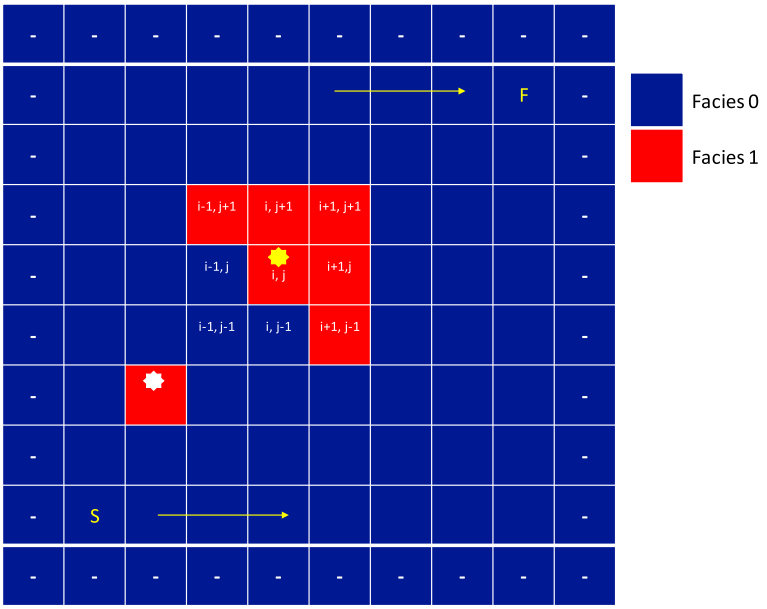

FIGURE A3 Example of cellular automaton simulation step displaying the occupant (red cell annotated with yellow star) that "survives" until the next iteration and the one (red cell annotated with white star) which "dies". The direction of traversal is indicated by yellow arrow(s)

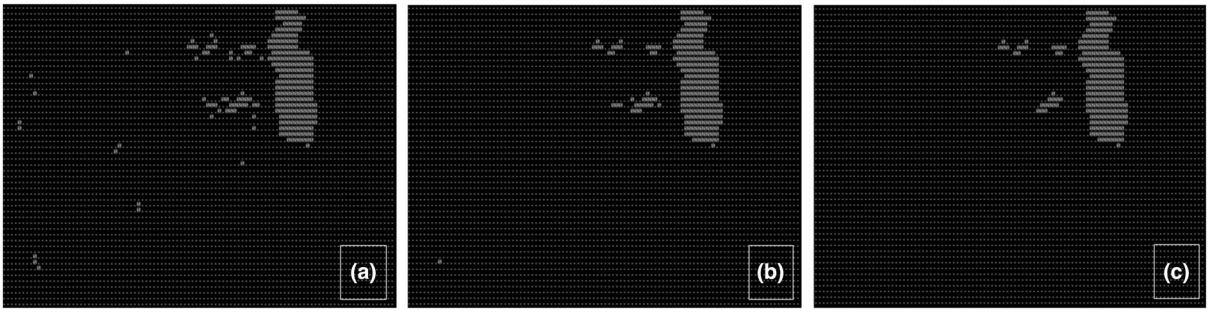

FIGURE A4 Graph illustrating the cleaning procedure of the cellular automaton algorithm using a set of rules (see text for more details) for the P10 case. Zeros correspond to "populated" cells and dots to "unpopulated" ones. Shape convergence in this example is achieved after two iterations. Initial and final states in (a) and (c), respectively

Delta-lobe extraction by cellular automata

A cellular automaton is a simulation technique that traverses the grid cell nodes and modifies node (grid cell) states based on a set of rules governed by the current states of the neighbouring cells (Feynman, 1982; Von Neumann, 1966; Wolfram, 2002). In the current study, the set of rules was assigned with the aim to preserve the emerged delta-lobe unit and discard stranded cells in the upstream part of the sediment dispersal system. A "populated" grid cell "survives" if the number of "populated" neighbouring cells is >= 4 (Figure A3). An "unpopulated" one is "reborn" in the presence of more than seven "populated" grid cells. This operation allows the merging of "unpopulated" inter-distributary depositional sites with the body of the fluvio-deltaic lobe to define its final shape (Figure A4).